

**INVESTIGATIONS OF NEW HORIZONS ON H₂/O₂ PROTON EXCHANGE
MEMBRANE FUEL CELLS**

**A THESIS SUBMITTED TO
THE GRADUATE SCHOOL OF NATURAL AND APPLIED SCIENCES
OF
THE MIDDLE EAST TECHNICAL UNIVERSITY**

BY

AHMET ÖZGÜR YAZAYDIN

**IN PARTIAL FULFILLMENT OF THE REQUIREMENTS FOR THE DEGREE OF
MASTER OF SCIENCE**

**IN
THE DEPARTMENT OF CHEMICAL ENGINEERING**

JULY 2003

Approval of the Graduate School of Natural and Applied Sciences

Prof. Dr. Canan ÖZGEN
Director

I certify that this thesis satisfies all the requirements as a thesis for the degree of Master of Science.

Prof. Dr. Timur DOĞU
Head of Department

This is to certify that I have read this thesis and that in my opinion it is fully adequate, in scope and quality, as a thesis for the degree of Master of Science.

Prof. Dr. Lemi TÜRKER
Co-Supervisor
Examining Committee Members

Prof. Dr. İnci EROĞLU
Supervisor

Prof. Dr. Işık ÖNAL

Assoc. Prof. Dr. Gürkan KARAKAŞ

Dr. Can APAK

Prof. Dr. Lemi TÜRKER

Prof. Dr. İnci EROĞLU

ABSTRACT

INVESTIGATIONS OF NEW HORIZONS ON H₂/O₂ PROTON EXCHANGE MEMBRANE FUEL CELLS

YAZAYDIN, Ahmet Özgür

M.S., Department of Chemical Engineering

Supervisor: Prof. Dr. İnci EROĞLU

Co-Supervisor: Prof. Dr. Lemi TÜRKER

July 2003, 96 pages

Proton exchange membrane fuel cells are electrochemical devices which convert the chemical energy of hydrogen into electrical energy with a high efficiency. They are compact and produce a powerful electric current relative to their size. Different from the batteries they do not need to be recharged. They operate as long as the fuel is supplied. Fuel cells, therefore, are considered as one of the most promising options to replace the conventional power generating systems in the future.

In this study five PEMFCs; namely EAE1, AOY001, AOY002, AOY003 and AOY004 were manufactured with different methods and in different structures. A test station was built to make the performance tests. Performances of the PEMFCs were compared by comparing the voltage-current (V-i) diagrams obtained during the initial tests at 25 ° C of fuel cell and gas humidification temperatures. AOY001 showed the best performance among all PEMFCs with a current density of 77.5 mA/cm² at 0.5 V and it was chosen for further parametric studies where the effect of different flow rates of H₂ and O₂ gases, gas humidification and fuel cell temperatures on the performance were investigated.

It was found that increasing fuel cell and gas humidification temperatures increased the performance. Excess flow rate of reactant gases had an adverse effect on the performance. On the other hand increasing the ratio of flow rate of oxygen to hydrogen had a positive but limited effect. AOY001 delivered a maximum current density of 183 mA/cm² at 0.5 V. The highest power obtained was 4.75 W.

Keywords: Fuel cell, proton exchange membrane, hydrogen, energy conversion

ÖZ

H₂/O₂ PROTON DEĞİŞİM ZARLI YAKIT HÜCRELERİNDE YENİ UFUKLARIN ARAŞTIRILMASI

YAZAYDIN, Ahmet Özgür

Y. L., Kimya Mühendisliği Bölümü

Tez yöneticisi: Prof. Dr. İnci EROĞLU

Ortak tez yöneticisi: Prof.Dr. Lemi TÜRKER

Temmuz 2003, 96 sayfa

Proton deęişim zarlı yakıt hücreleri (PDZYH) hidrojen gazının kimyasal enerjisini yüksek bir verimle elektrik enerjisine çeviren elektrokimyasal aygıtlardır. Boyutlarına göre yüksek elektrik akımı üretme gücüne sahip, küçük ve hafif yapıdadırlar. Pillerden farklı olarak şarj edilmeye ihtiyaç duymazlar. Yakıt beslendięi sürece çalışmaya devam ederler. Bu sebeplerden ötürü yakıt hücreleri günümüzde kullanılagelen güç üretim sistemlerinin gelecekteki en umut veren alternatifi olarak görölmektedir.

Bu çalışmada sırasıyla EAE1, AOY001, AOY002, AOY003 ve AOY004 adında beş adet PDZYH deęişik metotlar kullanılarak birbirlerinden farklı

yapılarda imal edilmiştir. Performans testlerini gerçekleştirmek için bir test istasyonu kurulmuştur. İmal edilen PDZYH'lerin performansları 25 °C yakıt hücresi ve gaz nemlendirme sıcaklıklarında elde edilen karakteristik voltaj-akım (V-A) eğrileri kullanılarak karşılaştırılmıştır. Bu karşılaştırma sonucu 0.5 V'ta 77.5 mA/cm²'lik bir akım yoğunluğu üreten AOY001'in en iyi performansı gösterdiği belirlenmiş ve AOY001 ileri aşamalarda yapılacak olan; H₂ ve O₂ gazlarının debileri ile yakıt hücresi ve gaz nemlendirme sıcaklıklarının performansa etkilerinin araştırılacağı parametrik çalışmalar için seçilmiştir.

Yapılan deneyler sonucunda yakıt hücresi ve gaz nemlendirme sıcaklıklarındaki artışın performansı arttırdığı gözlenmiştir. Reaksiyona giren gazların yüksek debi ile beslenmesi durumunda performansın bundan olumsuz yönde etkilendiği tesbit edilmiştir. Bunun yanı sıra oksijen gazının debisinin hidrojen gazının debisine oranı arttıkça performansın bir dereceye kadar arttığı gözlenmiştir. AOY001 0.5 V'ta maksimum 183 mA/cm² akım yoğunluğu vermiştir. Ulaşılan en yüksek güç değeri ise 4.75 W'dır.

Anahtar sözcükler: Yakıt hücresi, proton değişim zarı, hidrojen, enerji çevrimi

For always being there

Wherever may life land me

I dedicate this work to my grandfather Salih Aras

ACKNOWLEDGEMENTS

I would like to express my strongest thankfulness and respect to my supervisor Prof. Dr. İnci Erođlu for her guidance, patience and humanity throughout my graduate study. I am indebted her too many things but most because of being always beside me. She treated me sometimes like a sister sometime like a mum.

I am also indebted to Prof. Dr. Lemi Türker who offered suggestions and comments. His scientific approach as he does to every phenomenon added a significant value to this manuscript.

Thanks are due to EAE Elektrik A.Ş. for funding the project and supporting me financially. I am especially grateful to Örsçelik Balkan, CEO of EAE Group, who always backed me during my graduate study and let me benefited from his diverse experience. I am also thankful to Yusuf Hikmet Kaya, president of EAE Group.

All the technicians of Chemical Engineering Department, especially Süleyman Kuşhan, are appreciated for their help and continuous positive attitude. I also would like to thank to my friends Ahmet Aslanođlu, Sarp Kaya, Evren Güner, Ela Erođlu from the department and Mehmet Tansu Tunç from METU-BİLTİR for their help and support during my studies. My colleagues from EAE Elektrik A.Ş., Mesut Gündođdu, Varol Tanış, Gökhan Yıldırım and Vedat Voşki also deserve many thanks for their help. My special thanks go to Prof. Beycan İbrahimođlu from MSB-ARGE who donated the spraying gun and helped me to develop spraying method. I thank to Prof. Dr. Hayrettin Yücel for opening a space in his lab for me and giving the compressor and being always so warm to me. Finally I can't help myself to mention Dr. Can Apak, a 1969 METU, CHE Department graduate whom I met at the final stage of my project and experienced that even there is more than 30 years between us a METU graduate is always a METU graduate and different from all others. Many thanks to him for changing my vision. If I don't become an academician or I become semi engineer semi academician, he will be responsible for this. This work was supported by TUBİTAK MİSAG Project No: 230.

TABLE OF CONTENTS

| | |
|---|------|
| ABSTRACT..... | iii |
| ÖZ..... | v |
| DEDICATION..... | vii |
| ACKNOWLEDGEMENTS..... | viii |
| TABLE OF CONTENTS..... | ix |
| LIST OF TABLES..... | xii |
| LIST OF FIGURES..... | xiii |
| LIST OF SYMBOLS..... | xv |
| CHAPTER | |
| 1. INTRODUCTION..... | 1 |
| 1.1 Types of fuel cells | 4 |
| 1.1.1 Alkaline fuel cell (AFC)..... | 4 |
| 1.1.2 Phosphoric acid fuel cell (PAFC)..... | 5 |
| 1.1.3 Molten carbonate fuel cell (MCFC)..... | 5 |
| 1.1.4 Solid oxide fuel cell (SOFC)..... | 6 |
| 1.1.5 Proton exchange membrane fuel cell (PEMFC)..... | 6 |
| 1.2 Significance of the present work and its objectives..... | 7 |
| 2. LITERATURE SURVEY..... | 10 |
| 2.1 Proton exchange membrane fuel cell..... | 10 |
| 2.1.1 How does a PEMFC work?..... | 11 |
| 2.2.2 Function and structure of the basic components of a PEMFC..... | 12 |
| 2.2 Commercial PEMFCs | 16 |
| 2.3 Membrane electrode assembly | 19 |
| 2.4 Gas diffusion layer | 21 |
| 2.5 Gas distribution channels..... | 22 |
| 2.6. Humidification and water management..... | 25 |
| 2.7. Thermodynamics of PEMFCs..... | 27 |

| | |
|--|----|
| 2.8. Fuel cell irreversibilities and causes of voltage loss..... | 29 |
| 2.8.1 Activation losses..... | 32 |
| 2.8.1.1 The Tafel equation..... | 32 |
| 2.8.1.2 Reducing the activation overvoltage..... | 38 |
| 2.8.2 Fuel Crossover and internal currents..... | 39 |
| 2.8.3 Ohmic losses | 42 |
| 2.8.4 Mass transport or concentration losses | 43 |
| 2.9 Efficiency of a fuel cell..... | 47 |
| 3. EXPERIMENTAL..... | 49 |
| 3.1 Building test station | 49 |
| 3.2 Construction of fuel cells | 51 |
| 3.2.1 Materials used to construct the fuel cells..... | 52 |
| 3.2.1.1. Casing..... | 52 |
| 3.2.1.2. Current collectors..... | 53 |
| 3.2.1.3. Gas distribution plates..... | 53 |
| 3.2.1.4. Gas diffusion layers..... | 53 |
| 3.2.1.5 Membrane electrode assemblies (MEA) | 54 |
| 3.2.2. Methods used to manufacture gas diffusion layers and MEAs... | 54 |
| 3.2.2.1. Rolling method..... | 54 |
| 3.2.2.2. Spraying method..... | 55 |
| 3.2.3. Geometry of the gas distribution channels..... | 56 |
| 3.3 Experimental procedure..... | 58 |
| 3.4 Scope of the work..... | 59 |
| 4. RESULTS and DISCUSSION..... | 62 |
| 4.1. Comparison of the constructed PEMFCs | 62 |
| 4.2 Effect of operating conditions on the performance of the PEMFCs..... | 64 |
| 4.2.1 Effect of gas humidification temperature..... | 65 |
| 4.2.2 Effect of fuel cell temperature..... | 65 |
| 4.2.3 Effect of oxygen to hydrogen ratio..... | 68 |
| 4.3 Power and efficiency of the AOY001..... | 68 |
| 4.4 Comparison of the performances with literature..... | 71 |
| 4.5 Discussions..... | 72 |
| 5. CONCLUSION AND RECOMMENDATIONS..... | 78 |
| REFERENCES..... | 82 |

| | |
|---|----|
| APPENDICES..... | 85 |
| A. Sample Calculation For Fuel Cell Power..... | 85 |
| B. V-i Diagrams of Parametric Experiments of AOY001..... | 86 |
| C. V-i Diagram of Ion-Power's MEA Tested by Fuel Cell Energy..... | 96 |

LIST OF TABLES

TABLES

| | |
|--|----|
| 1.1 The advantages and disadvantages of fuel cells..... | 3 |
| 1.2 Different fuel cell types..... | 4 |
| 2.1 i_0 for the hydrogen electrode for various metals, for an acid electrolyte.. | 37 |
| 2.2 Cell voltages at low current densities..... | 42 |
| 3.1 Properties of the PEMFCs constructed..... | 60 |
| 3.2 Scope of the experiments..... | 61 |
| 4.1 OCVs and current densities of the constructed PEMFC..... | 63 |
| A.1 Power values for AOY001..... | 85 |
| B.1 Effect of humidification temperature with excess flow rate of gases..... | 86 |
| B.2 Effect of humidification temperature..... | 88 |
| B.3 Effect of fuel cell temperature with high level of humidification..... | 91 |
| B.4 Effect of fuel cell temperature with low level of humidification..... | 92 |
| B.5 Effect of O ₂ to H ₂ ratio..... | 94 |

LIST OF FIGURES

FIGURES

| | |
|--|----|
| 1.1 Comparison of conversion processes in the thermal power plants and fuel cells..... | 2 |
| 2.1 A schematic of a PEMFC membrane electrode assembly (MEA)..... | 12 |
| 2.2 A schematic representation of the PEM fuel cell cross-section consisting gas distribution channels (layers S and T), gas-diffusion layers (layers D and E), catalyst layers (layers A and C), and the PEM (layer B)..... | 14 |
| 2.3 Examples of different flow fields used in PEMFCs..... | 23 |
| 2.4 The different water movements to, within and from the electrolyte of a PEMFC..... | 27 |
| 2.5.a Graph showing the voltage for a typical low temperature, air pressure fuel cell..... | 30 |
| 2.5.b Graph showing the voltage for a typical air pressure fuel cell operating at about 800 °C. | 30 |
| 2.6 Tafel plots for slow and fast electrochemical reactions..... | 33 |
| 2.7 Graphs of cell voltage against current density, assuming all losses due only to the activation overvoltage at one electrode, for exchange current density i_0 values of 0.01, 1.0 and 100 mA cm ⁻² | 36 |
| 2.8 Graph showing the fuel cell voltage modelled using activation and fuel crossover/internal current losses only..... | 40 |
| 3.1 Test station..... | 50 |
| 3.2 General structure of the PEMFCs constructed..... | 52 |
| 3.3 Serpentine flow pattern..... | 57 |
| 3.4 Interdigitated flow pattern..... | 58 |
| 4.1 Performance comparison of the PEMFCs constructed..... | 63 |

| | |
|--|----|
| 4.2 Effect of gas humidification temperature with excess flow rate of reactants. (T Cell = 50 °C; H ₂ : 0.4 sLm; O ₂ : 0.2 sLm)..... | 66 |
| 4.3 Effect of gas humidification temperature (T Cell = 50 °C; H ₂ : 0.1 sLm; O ₂ : 0.05 sLm)..... | 66 |
| 4.4 Effect of cell temperature at high humidification level (T Hum = T Cell + 10 °C; H ₂ : 0.1 sLm; O ₂ :0.05 sLm)..... | 67 |
| 4.5 Effect of cell temperature at low humidification level (T Hum = T Cell - 5 °C; H ₂ : 0.1 sLm; O ₂ : 0.05 sLm)..... | 67 |
| 4.6 Effect of O ₂ to H ₂ ratio (T Cell = 60 °C; T Hum = 70 °C; H ₂ : 0.1 sLm)..... | 69 |
| 4.7 Power and voltage-total current curve of AOY001 (T Cell = 60 °C; T Hum = 70 °C; H ₂ : 0.1 sLm O ₂ : 0.1 sLm)..... | 70 |
| 4.8 Comparison of the V-i curves provided by Ion-Power and obtained in this study of the MEA used in AOY001..... | 72 |
| C.1 V-i diagram of purchased MEA from Ion-Power..... | 96 |

LIST OF SYMBLOS

| | |
|----------------|--|
| A | coefficient in Tafel equation, also area |
| a | activity |
| B | coefficient in equation for mass transport voltage loss |
| E | EMF or open circuit voltage |
| E^0 | EMF at standard pressure |
| F | Faraday constant, 96485 coulombs |
| G_f | Gibbs free energy of formation |
| ΔG_f | change in Gibbs free energy of formation |
| ΔG_f^0 | change in Gibbs free energy of formation at standard pressure |
| ΔH_f | change in enthalpy of formation |
| I | current |
| i | current density |
| i_0 | exchange current density at an electrode/electrolyte interface |
| i_l | limiting current density |
| i_n | value of this internal current density |
| N | Avogadro's number, 6.022×10^{23} |
| P | pressure or partial pressure of the gas |
| P^0 | standard pressure at standard pressure |
| R | universal gas constant, $8.314 \text{ J K}^{-1} \text{ mol}^{-1}$, also electrical resistance |
| r | area-specific resistance |

| | |
|--------------------|--|
| T | temperature |
| V | voltage |
| V_c | actual operating voltage of a single fuel cell |
| ΔV | voltage change |
| ΔV_{act} | voltage drop due to activation over voltage |
| ΔV_{ohm} | voltage drop due to ohmic losses |
| ΔV_{trans} | voltage drop due to mass transport losses |
| α | charge transfer coefficient |

CHAPTER 1

INTRODUCTION

Hydrogen fuel cells are electrochemical devices which convert chemical energy of hydrogen directly to electrical energy. They are highly efficient and low emission power generating systems. Hydrogen is electrochemically oxidized within the fuel cell. During this oxidation reaction electrical current is drawn basically by forcing the electrons to flow through a conductor to complete their oxidation process. In usual electrical power generating systems combustion of fuel produces heat and this heat is converted to mechanical energy. Finally mechanical energy is utilized to generate electricity. In fuel cells systems, however, instead of this procedure, which has three steps, chemical energy of fuel is directly converted to electricity in only one step. Figure 1.1 demonstrates the conversion process taking place in usual thermal power generating systems and fuel cells. Therefore, efficiency of a fuel cell is not subject to the restriction of Carnot processes. Under practical conditions fuel cells have demonstrated 50% of electrical energy efficiencies. On the other hand, with an internal combustion engine the maximum electrical energy efficiency that can be obtained is around 15-20% (Tomantschger et.al., 1986). Moreover in large system (> 5 kW) if heat produced by the fuel cell is recovered, which is called cogeneration total energy efficiency of a fuel cell may reach up to 80%. Different from the

batteries they do not need to be recharged. They operate as long as the fuel is supplied. Since a fuel cell utilizes hydrogen, it is an environmental friendly technology. They have a modular structure since they have no moving parts.

Fuel cells, therefore, are considered as one of the most promising options to replace the conventional power generating systems in the future. Due to these favorable properties fuel cells have found a wide range of application areas from

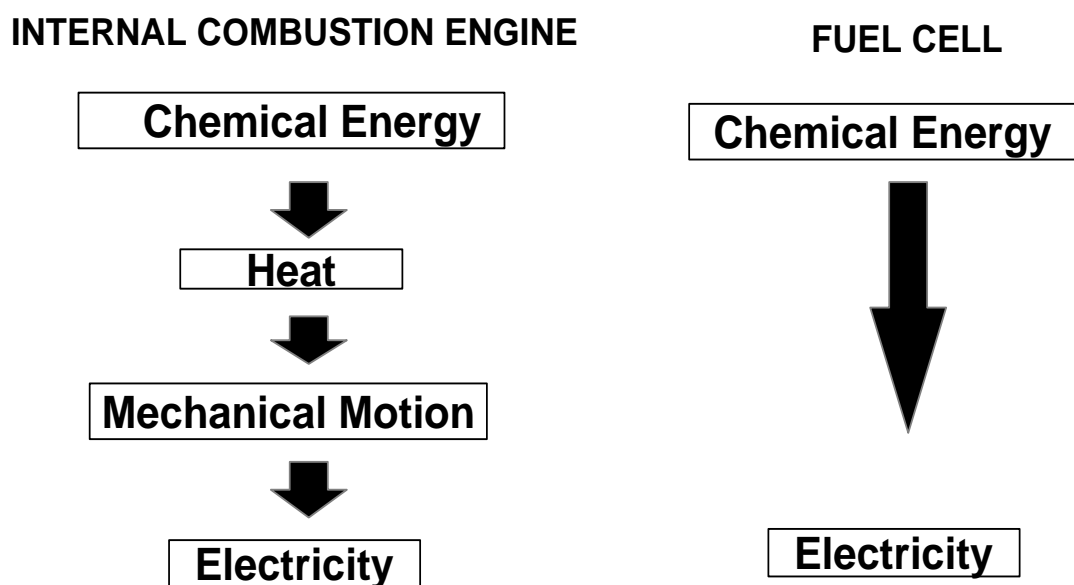


Figure 1.1 Comparison of conversion processes in the thermal power plants and fuel cells

large stationary power applications to power small electronic equipments. Today fuel cells have been demonstrated successfully in hospitals, parks, and apartments where huge amounts of electrical energy is needed, automobiles, busses and bicycles where modularity and weight is a concern and small electronic equipments such as cellular phones where high technology rules. (Larminie et.al., 2003)

Although much research and development has been done on fuel cells recently, there are still some problems waiting to be solved. The major problem

in front of fuel cells is their high initial costs. Advanced materials used in the fuel cells are expensive and prices are not expected to fall until the mass production of the fuel cells is realized. Advantages and disadvantages of the fuel cells are tabulated in Table 1.1.

Table 1.1 The advantages and disadvantages of fuel cells

| |
|--|
| <p style="text-align: center;">Advantages</p> <ul style="list-style-type: none">• Electrical efficiency is high• The pollution level is low and is zero when pure hydrogen is used as fuel• There is only a small number of moving parts• The noise level is low• The maintenance cost is low• Low cost fuels can be used with high temperature systems• Cogeneration of heat arises the efficiency significantly |
| <p style="text-align: center;">Disadvantages</p> <ul style="list-style-type: none">• High initial cost of the system• Large volume and weight fuel storage systems are needed• Clean hydrogen is presently high priced• Life times are not known precisely |

1.1. Types of fuel cells

There are five different types of fuel cells. The main difference between them is the electrolyte used. Besides this, operating temperatures of the fuel cells is another distinction which determines the application areas of the fuel cells. Table 1.2 shows the differences between fuel cell types.

Table 1.2 Different fuel cell types

| Fuel cell type | Alkaline | Phosphoric acid | Proton exchange membrane | Molten carbonate | Solid oxide |
|----------------------------|-----------------|--------------------------------|--------------------------|-------------------------------|-----------------|
| Operating temperature (°C) | 80 | 200 | 80 | 650 | 700-1000 |
| Electrolyte type | KOH | H ₃ PO ₄ | Solid polymer | Molten salt | Ceramic |
| Ion transferred | OH ⁻ | H ⁺ | H ⁺ | CO ₃ ²⁻ | O ²⁻ |
| Startup time | Minutes | Minutes | Seconds | >10 hours | > 10 Hours |

1.1.1 Alkaline fuel cell (AFC)

Alkaline fuel cells have been used since the mid-1960s by NASA in the Apollo and space shuttle programs, to power electrical systems on spacecrafts. They were considered appropriate for small scale aerospace and defense applications.

However, their use in commercial applications is limited because they must operate with pure hydrogen and with pure oxygen, or air from which the carbon dioxide has been removed since the electrolyte used is KOH. (Kordesch et.al., 1996)

1.1.2 Phosphoric acid fuel cell (PAFC)

Phosphoric acid fuel cells have been field tested since the 1970s. They are the most developed fuel cell technology for stationary power applications, with existing installations in buildings, hotels, hospitals, and electric utilities in Japan, Europe, and the United States. The principal use of these systems is expected to be mid-to-large stationary power generation applications. However, the corrosive liquid electrolyte and high operating temperature (200 degrees Celsius) require complex system design and negatively impact operating life and cost. (Kordesch et.al., 1996)

1.1.3 Molten carbonate fuel cell (MCFC)

Molten carbonate fuel cells operate at very high temperatures (650 degrees Celsius) that allow them to use fuel directly without the need for a fuel processor. Their system design is more complex than phosphoric acid fuel cells due to their higher operating temperature and their utilization of a molten electrolyte. They require significant time to reach operating temperature and to respond to changes in electricity demand, and therefore are best suited for the provision of constant power

in large utility applications. They have been built in small numbers in the United States and Japan and a prototype 1.8-megawatt power plant has been demonstrated in the United States. (Kordesch et.al., 1996)

1.1.4 Solid oxide fuel cell (SOFC)

Solid oxide fuel cells operate at extremely high temperatures (700 degrees Celsius - 1,000 degrees Celsius). As a result, they can tolerate relatively impure fuels, such as those obtained from the gasification of coal. Their relatively simple design (because of the solid electrolyte and fuel versatility), combined with the significant time required to reach operating temperature and to respond to changes in electricity demand, make them suitable for large to very large stationary power applications. They have been demonstrated in laboratory settings and in early field trials. (Larminie et. al., 2003)

1.1.5 Proton exchange membrane fuel cell (PEMFC)

Proton exchange membrane fuel cell (PEMFC) uses solid polymer membrane (a thin plastic film) as an electrolyte. They are compact and produce a powerful electric current relative to their size. The first practical application for PEM fuel cells was in the Gemini space program. Most automakers believe that PEM fuel cells are the only fuel cell appropriate for providing primary power on-board a

vehicle. PEM fuel cells deliver higher power density, resulting in reduced weight, cost and volume and improved performance. An immobilized electrolyte also simplifies sealing in the production process, reduces corrosion, and provides for longer cell and stack life. PEM fuel cells operate at low temperatures (less than 100 degrees Celsius), allowing faster start-ups and immediate responses to changes in the demand for power. They are ideally suited for transportation and smaller stationary applications. PEM fuel cells have been demonstrated in systems ranging in size from 1 watt to 250 kW. (Larminie et. al., 2003)

1.2 Significance of the present work and its objective

Entering the new millennium, world's main energy source fossil fuels (i.e., petroleum, natural gas and coal), which meet most of the world's energy demand today, are being depleted rapidly. Also, their combustion products are causing global problems, such as the greenhouse effect, ozone layer depletion, acid rains and pollution, which are posing great danger for our environment, and eventually, for the total life on our planet. Besides this aspect we are witnessing wars and political challenges between nations to reign world's energy sources. Therefore; new, clean and renewable energy sources should be adopted our lives to be able to talk about a sustainable future.

Many engineers and scientists agree that the solution to all of these global problems would be to replace the existing fossil fuel system with the Hydrogen Energy System. Hydrogen is considered to be an ideal energy carrier in the

foreseeable future. It can be produced from water by using a variety of energy sources, such as solar, nuclear and fossil, and it can be converted into useful energy forms efficiently and without detrimental environmental effects. The only by-product is water. When solar energy - in its direct and/or indirect forms - is used to produce hydrogen from water, both the primary and secondary forms of energy become renewable and environmentally compatible, resulting in an ideal, clean and sustainable energy system - the Solar Hydrogen Energy System. Hydrogen, produced from renewable energy (solar) sources, would result in a permanent energy system which we would never have to change.

Hydrogen can be used in any application in which fossil fuels are being used today, with sole exception of cases in which carbon is specifically needed. Hydrogen can be used as a fuel in furnaces, internal combustion engines, turbines and jet engines, even more efficiently than fossil fuels, i.e., coal, petroleum and natural gas. Automobiles, buses, trains, ships, submarines, airplanes and rockets can run on hydrogen.

Enlightened with those facts, the importance of the fuel cell technology can be clearly understood to bring the hydrogen energy to our lives for a sustainable future. What we need is efficient energy converters and fuel cells are the strongest candidates for this purpose. All around the world a tremendous research facility is in progress about many different aspects of fuel cells. Both governmental and private sectors in the world have invested billions of dollars for research on fuel cells. Especially, two types of fuel cells; PEMFCs and SOFCs, are the ones which are the focus of most of the research facilities. The progress for PEMFCs is one step beyond the SOFCs since its application areas is more than they are for SOFC. Moreover,

the giants of automotive industry in the world are pushing for the development of PEMFCs which is the only suitable fuel cell type that can be used in vehicles. Today there is almost no automotive manufacturer which does not have research and development facility about fuel cell technology. Therefore, strong interest of automotive industry provided a rapid development of PEMFCs compared with other types of fuel cells.

Unfortunately, although there has been an extensive research facility all around the world, in Turkey there is no significant work done on PEMFCs. A lot of research progress should be performed to bring and apply this technology in our country. This is the first academic study completed on PEMFCs in Turkey. It has the importance of initiating further research facilities in METU and in our country. It contains the basics of fuel cell technology and many helpful hints and data for researchers.

The objective of this study was to manufacture PEMFCs operated by pure hydrogen and oxygen and to investigate the factors affecting their performance such as fuel cell temperature, humidification temperature of reactant gases and ratio and flow rate of reactant gases.

During this study PEMFCs which are different in structure were manufactured. A test station was constructed to do performance tests. Different manufacturing techniques for main components of a PEMFC were developed and applied. Performance and response of PEMFCs at different operating conditions were examined by voltage-current density data collected.

CHAPTER 2

LITERATURE SURVEY

2.1 Proton exchange membrane fuel cells

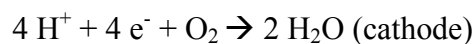
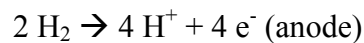
This work focuses on proton exchange membrane fuel cells (PEMFC). PEMFC technology was invented at General Electric in the early 1960s, through the work of Thomas Grubb and Leonard Niedrach. PEM technology served as part of NASA's Project Gemini in the early days of the U.S. piloted space program. Batteries had provided spacecraft power in earlier Project Mercury missions, but the lunar flights envisioned for Project Apollo required a longer duration power source. Project Apollo mission planners; however, chose to use alkaline fuel cells for both the command module and lunar modules, as did the designers of Space Shuttle a decade later due to the robustness of the technology. It wasn't until the incorporation of Nafion (proton conducting membrane commercialized by DuPont in the early 1970s) into the PEM fuel cell that work on this technology began to emerge.

By the end of 1970s, technical and economic barriers still prevented the development of a competitive fuel cell product. In 1984, the Office of Transportation Technologies at the U.S. Department of Energy began to fund the development of the

various fuel cell types, including PEMFCs. In the last decade, the cost and size of fuel cell systems have decreased by over 90%, while performance and endurance continue to rise (Haug, 2002).

2.2.1 How does a PEMFC work?

This type of fuel cell derives its name from the proton exchange membrane that acts as the electrolyte. On either side of the membrane is a catalyst-containing electrode on which the following reactions occur:



As shown in Figure 2.1, hydrogen gas is split to its protons and electrons at the catalyst layer; the proton exchange membrane allows protons to pass from the anode to the cathode side, while preventing gases from diffusing from one side to the other side. Electrons travel to the cathode through the external circuit producing the electrical current. At the cathode; aided by electrode potential, the protons and electrons recombine with O_2 at the catalyst surface to form water. Membrane coated with catalyst containing electrodes is called membrane electrode assembly (MEA) where the electrochemical reaction takes place.

2.2.2 Function and structure of the basic components of a PEMFC

A PEMFC may be divided into four main parts. Figure 2.2 shows a detailed illustration of a PEMFC.

The MEA (layers A, B and C) are placed between the gas-diffusion layers (layers D and E) and they are all sandwiched between two graphite plate current

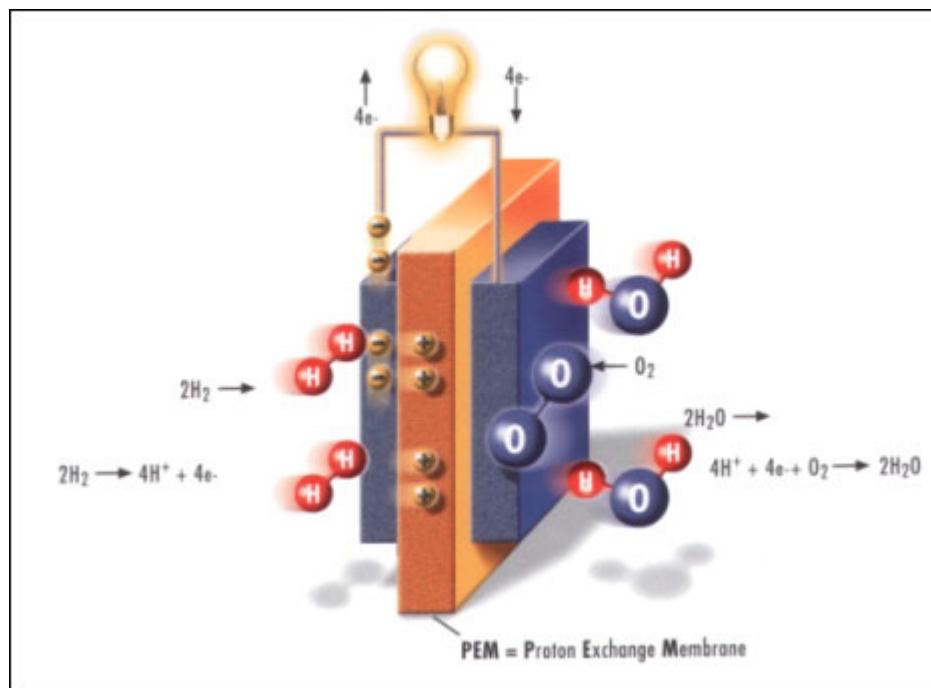


Figure 2.1 A schematic of a PEMFC membrane electrode assembly (MEA)

collectors, with machined microchannels (layers S and T), as in microchannel reactors (Tonkovich, 1999), for gas distribution.

The gas-diffusion layer (GDL) (layers D and E) serves as the electron collector and a permeator for reactant gases as well as for liquid water. The PEM (layer B) requires water for effective proton transport, which limits the practical operating temperature of atmospheric fuel cells to about 80°C (when water

vapor pressure is roughly half an atmosphere). However, if the pores of the gas-diffusion layers get filled with liquid water, transport of oxygen and hydrogen to the catalyst layers is impeded, severely

limiting the fuel cell performance. This is avoided by imparting hydrophobicity to the gas-diffusion layers to allow gas and liquid phases to co-exist within pores. The gas-diffusion backing typically involves a carbon cloth, about 350 μm in thickness and woven from carbon fibers, on the one side of which the catalyst layer is deposited. The carbon cloth is treated with 40–70 wt.% poly-tetrafluoroethylene (PTFE, e.g., Teflon®) mixed with 10–20 nm carbon particles followed by sintering to melt the PTFE and coat the carbon fibers (Paganin, 1996) and rendering it quite hydrophobic. The initial porosity of the carbon cloth is 70–80%, but its finished porosity is 55–65%.

The catalyst layer is 5–50 μm in thickness and contains Pt microcrystallites, roughly 2–4 nm in diameter, supported on the surface of largely non-porous carbon black particles, around 30 nm in diameter, at a Pt/C loading of about 20–40 wt.% and $\leq 0.4\text{mgPt}/\text{cm}^2$ of MEA area. The interstitial spaces among the carbon particles are filled with an ionomer (e.g., Nafion®) solution to allow proton transport (Raistric et.al., 1986), and occasionally with some PTFE, although the latter may not be necessary for thin catalyst layers (Wilson et.al., 1992). The deposition of the catalyst layer on the gas-diffusion electrode is accomplished by painting, spraying, or filtration, of the catalyst/ionomer dispersion. A polymer electrolyte membrane (e.g., Nafion® 115 or 117), 50–175 μm thick, is hot-pressed at a temperature slightly above its glass transition temperature between the two electrodes such that the catalyst layers are on either side of the membrane. Alternate fabrication

procedures are also employed (Wilson et.al., 1992).

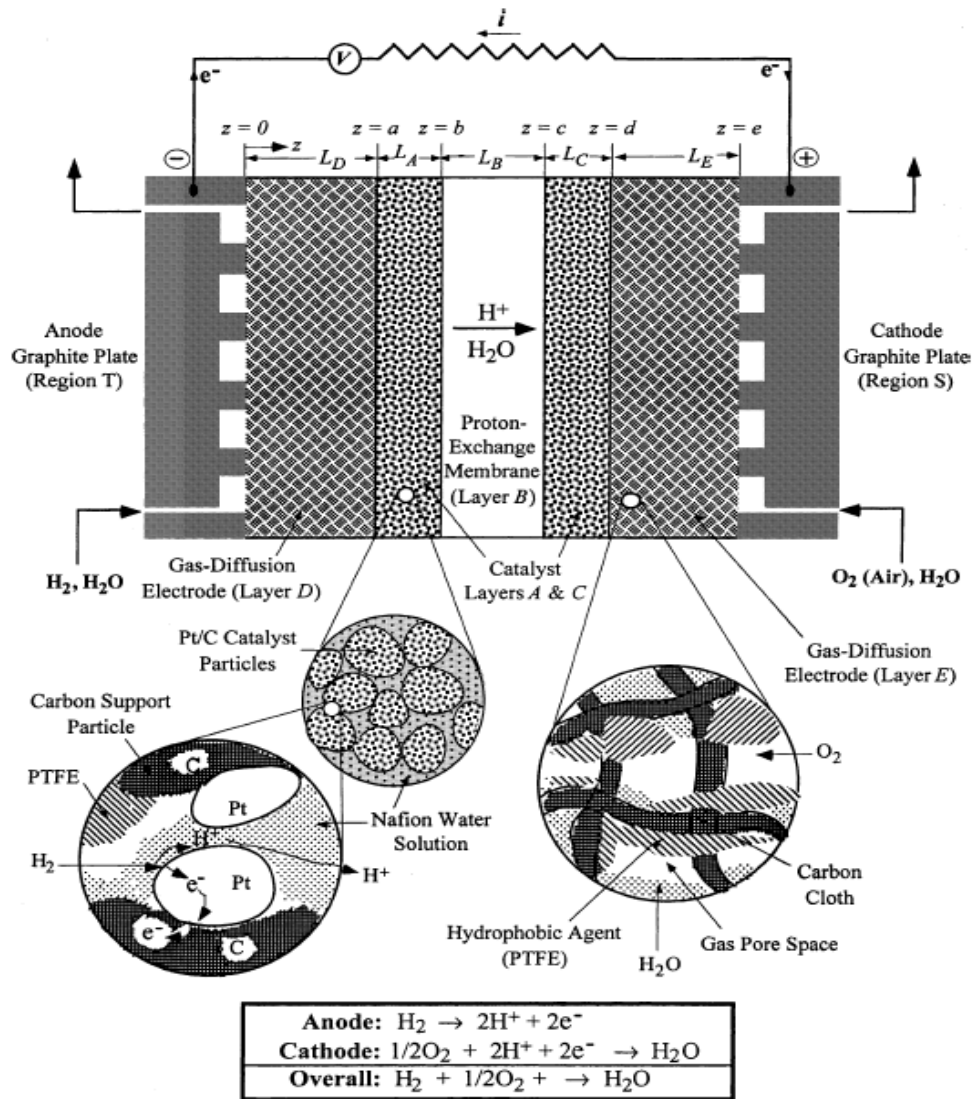


Figure 2.2 A schematic representation of the PEM fuel cell cross-section consisting gas distribution channels (layers S and T), gas-diffusion layers (layers D and E), catalyst layers (layers A and C), and the PEM (layer B). (Tamphan 2001)

The electrons produced at the anode catalyst surface are conducted via the carbon catalyst support and the carbon fibers of the gas-diffusion backing to the current collector and thence to the external circuit. The protons diffuse

through the ionomer solution within the catalyst layer and then through the PEM to arrive at the cathode. The catalyst layer is, thus, designed to maximize the interfacial area among its various phases, namely, the catalyst crystallites, the carbon support, the hydrophilic region consisting of ionomer, and any hydrophobic region containing Teflon®.

In addition to good interfacial contact among the layers, the continuity of the respective phases for electronic and protonic conduction is also essential. If there is too little ionomer, for instance, the proton conduction pathway will be fragmented. On the other hand, too much ionomer could compromise electronic conductivity by further distancing the carbon particles and increasing the path length for proton conduction.

The perfluorosulfonic acid membranes such as Nafion® produced by Du Pont (and similar membranes produced by Dow, W.L. Gore, and Asahi Glass) consist of a fluorocarbon, Teflon®-like, backbone with side-chains culminating in –SO₃H groups. In the presence of water, these sulfonic acid groups dissociate, forming hydronium ions (Grot, 1989) responsible for proton conduction. There are many studies on the nanostructural aspects of the Nafion® membranes. Based on small angle X-ray diffraction and other characterization studies, Gierke and co-workers (1981) proposed in their “cluster-network model” that the incompatibility of the fluorocarbon and the hydrophilic phase leads to the formation of inverted micelles, 3–5 nm in diameter, which are interconnected through short narrow channels, 1–2 nm in diameter, to provide a network for proton diffusion interspersed throughout the fluorocarbon matrix. The conductivity of Nafion® is extremely sensitive to relative humidity (RH), being essentially an insulator below a threshold of about 10%

RH and rising through several orders of magnitude to about 0.07 S/cm at 80 °C and 100% RH (Tamphan, 2000). The mechanism involving ordinary diffusion and Grotthus chain conduction explaining high proton conductivity in aqueous solutions is discussed by Glasstone et al. (1941) and Bockris and Reddy (1970). Nafion® also deters short-circuiting of electrons, as well as cross-over of reactants, its permeability of H₂ and O₂ being of the order of only 10⁻¹⁰ mol/cm² s atm (Gottesfeld, 1998).

2.2 Commercial PEMFCs

In general, a single PEM fuel cell has no practical importance due to its low voltage. A stack of cells can be arranged in series to be utilized in many useful applications such as cars, buses, power plants, etc. The desired voltage determines the number of cells in the stack, while the power determines the size of active cell area.

Nowadays, PEM fuel cells are utilized in many different applications, such as stationary power plants in commercial building and development of zero emission - vehicles. Dr .F. Panik, who runs Daimler-Benz's fuel-cell program, foresees cleaner, fuel saving buses and cars such as Necar3 and the 40-foot ultramodern Nebus (electric bus) run by several stacks of fuel cells that; make electricity to drive the motors that turn the wheels without combustion. New labs and workshops that auto-maker Daimler-Benz is equipping for a top-priority fuel-cell development program could make the noisy, polluting piston engines that power: the world's cars, trucks, and buses as obsolete as the steam locomotive. This work is the most visible

evidence of an accelerating wave of R&D by auto-makers and component suppliers around the world that have committed more than \$1 billion to fuel cell power systems (Hoffman. 1996).

In an effort to take part in the latest development in the fuel cell powered vehicles, Ford Motor Co. is joining Germany's Daimler-Benz in an attempt to manufacture environmentally friendly vehicles by 2005, using advanced fuel cell technology which reduces both noise and emissions. Ford will invest around \$420 million in a partnership between Daimler and Ballard Power Systems, a Canadian fuel cell propulsion specialist. The investment, in the form of cash, technology and assets, will give Ford 15 percent of Ballard and 23 percent of DBB Fuel Cell Engines, a Daimler subsidiary which is working on the development of fuel cell systems. Further development of the technology could lead to the first cars powered by fuel cells being commercially available in 2005.

General Motors (GM) completed a three year effort in 1993, which demonstrated proof-of-feasibility for methanol-fueled proton exchange membrane (PEM) fuel cells as an electrochemical engine for transportation applications. In Phase I, stand-alone operation of a 10 kW PEM fuel cell system was achieved using real-world automotive components such as fluid injectors and pressure regulators. The GM program is currently completing Phase II, which will result in the demonstration of a 30-kW system. Advancements are being made in three areas: fuel processing, fuel cell stack, and system integration. The General Motors development team includes the General Motors Research and Development Center as prime contractor and several participating divisions of Delphi Automotive Systems, namely, Delphi Energy and Engine Management Systems (formerly AC

Rochester), Delphi Harrison, Delphi Packard, and Delco Electronics. Key subcontractors include DuPont and Ballard Power Systems (Rose, 1998).

In 1997 Chrysler's direct hydrogen fuel cell project (Pentastar) was completed. The fuel cell portion of the effort was performed by Allied Signal and was focused on a design-to-cost approach in which materials development plays a critical role. Low-cost bipolar plates and low cost membranes have been developed. A 6-kW stack was fabricated and durability testing of low-cost bipolar plate materials was completed. Chrysler Libeny, Allied Signal Aerospace, Allied Signal Automotive, and Allied Signal Research and Technology supported Pentastar. In a similar manner, Toyota Company, which already sells a hybrid car in Japan, has a development program under way to involve some 200 researchers. Last year at two major auto shows, the company exhibited a version of its RAV4 sport-utility vehicle, equipped with a demonstration fuel-cell electric power train of its own design (Phillips, 1997).

In the underwater applications, recently, International fuel cell Corp. in Connecticut has successfully demonstrated a 10 kW prototype of a 20 kW fuel cell power plant designed to be installed in a 44 inch unmanned underwater vehicle. The power plant is based on a passive system concept requiring no circulation of gases for thermal management and minimal water management. The power plant was reported to have an energy efficiency of up to 68 percent (Schroll, 1994).

In space applications, PEM fuel cell would be the most suitable candidate to meet the needs of high power and efficiency and relatively small volume power sources. Today NASA's space shuttles each rely on a trio of 15-kilowatt fuel cells to generate onboard power and provide drinking water for the crew. Fuel cells

are the ideal power-generating device for a spacecraft like the shuttle, which is equipped with a supply of chemically pure hydrogen and oxygen (Appleby and Foulkes, 1989). The latest applications and interests in PEM fuel cells presented above are brief examples of the market demand concerning this new and important energy-generating source, which is expected to grow even bigger in the near future.

2.3 Membrane electrode assembly

Membrane electrode assembly (MEA) is considered to be the hearth of the fuel cell where the electrochemical reaction coupled with ion transport and mass transfer occurs. A detailed description of the MEA is given in section 2.1.2.

The proton exchange membrane allows ions to pass easily from the anode to the cathode, while preventing gases from diffusing from one side of the MEA to another. The standard industry membrane currently used is Nafion, first developed by DuPont more than 30 years ago. Similar membranes currently being used include Flemion (Asahi Glass Co., Japan), Aciplex (Asahi Chemical Industry Co., Japan) and a modified membrane PRIMEA developed by W. L. Gore & Associates, GmbH, Germany. Currently these membranes are made as thin as 25 microns, while still maintaining the structural stability needed to withstand pressure differences that may occur between the anode and cathode sides.

When the membrane is coated by a catalyst layer it is called membrane electrode assembly. Many different methods have been developed over the last decade describing procedures to manufacture MEAs for PEMFCs.

Fedkiw and Her (1992) describe a two step impregnation-reduction method in which the Nafion membrane undergoes an ion exchange reaction with a metal salt and then the impregnated membrane is exposed to a reductant in a second operation. Wilson (1993) prepares the catalyst layer separately and then hot-presses the two electrodes to the membrane forming the MEA. 20% Pt dispersed in carbon dissolved in 5% Nafion solution (in isopropyl alcohol) and glycerol to form an ink which is then applied to a Teflon blank and heated until dry, resulting in Pt supported on carbon with the Nafion acting both as a binder and a support. More layers of Pt/C/Nafion ink are added until the desired catalyst loading is achieved. The catalyst coated Teflon blanks are then hot pressed to the Nafion membrane resulting in the MEA. Using this method of catalyst loading, Wilson has reduced the Pt loading to 0.15 mg Pt/cm² with minimal loss in performance. Several others have used similar techniques to impregnate platinum supported particles into perfluorosulfonate ionomers (PFSI, such as Nafion) with the goal of maximizing the active surface area of the Pt and the contact between Pt and PFSI.

This method involves painting, spraying or printing of catalyst inks, is generally accepted as standard for MEA manufacture today. The three phase interface of electrolyte and carbon supported catalyst allows effective gas and water diffusion and proton transport and electron transport to and from the catalyst sites. Refinements of this process have involved optimizing the ratios of Pt, C and Nafion present in this three-phase interface. Uchida (1996) simplified the MEA construction method by simply applying ink to the gas diffusion layer (GDL). A pair of these electrodes/backings was then hot-pressed to the membrane. Results showed improved performance over the conventional method for Pt loading of

0.5 mg Pt/cm². The method was not tested for lower catalyst loadings. There are limitations on the catalyst activity imposed by the particle size of Pt on activated carbon.

As alternatives, electrodeposition and sputter deposition have been used to manufacture MEAs of low catalyst loadings. This technique has been shown to produce low-loading electrodes because of its ability to deposit catalyst in smaller particle sizes resulting in a more active catalyst per unit weight than traditional methods. Both pulse and direct current (DC) electrodeposition have been used to localize a thin layer of Pt near the surface of the MEA, resulting in the development of electrodes on the order of 0.05 mg Pt/cm². Verbrugge (1994) electrodeposited Pt from a dilute solution containing a Pt cation species. Sputter deposition is widely used for integrated circuit manufacturing and has been investigated for the preparation of more effective fuel cell electrodes for more than a decade.

2.4 Gas diffusion layer

Gas diffusion layer (GDL) is the porous backing layer, which is placed behind the catalyst layer, fulfills important tasks in the PEMFC. In this layer, combined requirements of effective reactant gas supply to the catalyst layer, effective water supply and removal in either vapor or liquid form have to be simultaneously fulfilled. Wet proofing by PTFE is required to ensure that at least part of the pore volume in the cathode backing remains free of liquid water in an operating cell. Obviously, the backing layer has to be made of a material of high and stable

electronic conductivity in a wet environment.

A common method of manufacturing the GDL was reported by Giorgi et al. (1998). For the preparation of the GDL a homogenous suspension was prepared by mixing and stirring in an ultrasonic bath at room temperature for 25 min the carbon with an appropriate amount of PTFE dispersion. The suspension was spray deposited on to a porous support. The layer was dried in air at 120 °C for 1 h, followed by a thermal treatment at 280 °C for 30 min to remove the dispersion agent contained in PTFE, and finally sintered at 350 °C for 30 min. Moreira et al. (2003) reported a similar method where a combination of pre-treated carbon paper and carbon cloth was used as backings. The pretreatment consisted of washing the backings in warm acetone, ethanol and ultra-pure water, during 30 min each, followed by drying at 80 °C during 30 min to eliminate all humidity, allowing better absorption of the mixture. Next, a mixture of activated carbon and PTFE in adequate quantities was applied on both faces of the backings and final structure were heated at 280 °C during 30 min under open air conditions, which allowed to remove the dispersion agents from the Teflon , and finally the sample was sintered at 330 °C during 30 min.

2.5 Gas distribution channels

Gas distribution channels are usually machined over the current collectors. Different flow field patterns for gas distributions were reported in the literature. A good summary of them is given in Larminie et al. (2003).

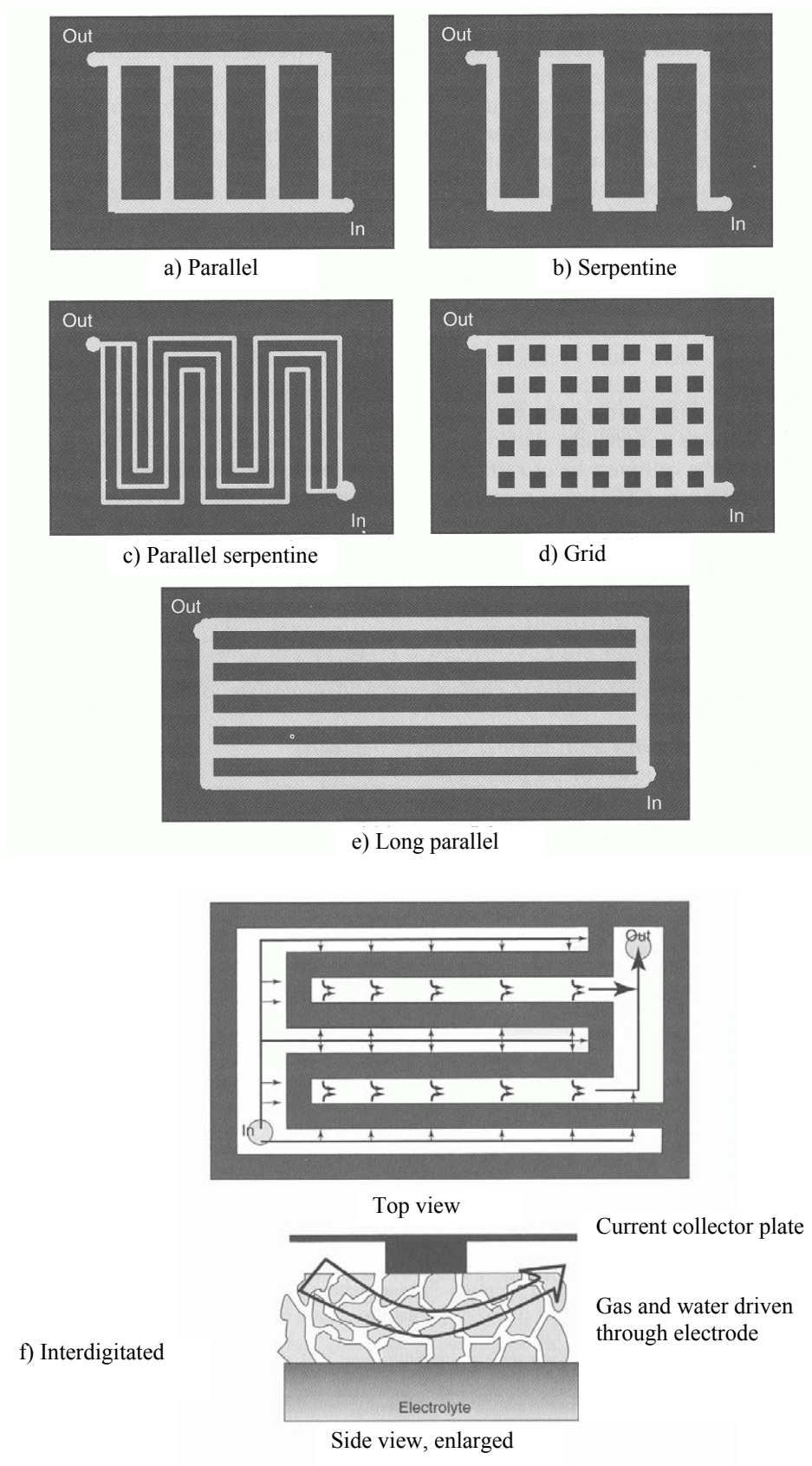


Figure 2.3 Examples of different flow fields used in PEMFCs

Examples of different flow field patterns used in PEMFCs are given in Figure 2.3. In Figure 2.3.a a parallel structure is shown. The supposed problem of parallel systems is that it is possible for water, or some reactant impurity such as nitrogen, to build up in one of the channels. The reactant gas will then quite happily move along the other channels, and the problem will not be shifted, leaving a region of the electrode unsupplied with reactants. This leads to the more serpentine systems such as Figure 2.3.b. Here it can be guaranteed that if the reactants are moving, they are moving everywhere, a blockage will be cleared. The problem with the serpentine systems is that the path length and the large number of turns mean that excessive work has to be done in pushing the gases through. The patterns such as Figure 2.3.c are something of compromise.

The pattern of Figure 2.3.d could be described as intensely parallel. The gases can swirl all over the face of the electrode. The idea is that any pockets of impure gases will be shifted by the swirling process of the probably unsteady flow of gas through the system. However, it would still be possible for water droplets to form, and not be shifted.

The grooves in the flow field are usually a little less than 1mm in width and height. In order water droplets not to form and stick in the channels, the system should be arranged so that the pressure drop along each channel is greater than the surface tension holding a water drop in place. That way, if the gas flow is stopped, there would be sufficient pressure to move the water droplet and get the gas moving again.

The pattern of Figure 2.3.e consists of long straight runs and the plate that the channels are machined is rectangular in form, not square, with the width several

times the height. This has the advantage of being straight with no inefficient bends and turns.

A significantly different flow pattern from others is shown in Figure 2.3.f called interdigitated flow field. Here the design forces the forces the reactant gases to blow the water through the cell and over the entire electrode. This is well described by Wood et al. (1998). Here the channels are like a maze with no exit. The gas is forced under the current collector plate and into the electrode, driving the water with it. If the flow field is well designed, this will happen all over the electrode. Good results are reported for this method, though the reactant gases must be driven at pressure through the cell.

2.6 Humidification and water management

It is clear from the description of a proton exchange membrane that there must be sufficient water content in the polymer electrolyte. The proton conductivity is directly proportional to the water content. The greatest danger posed by water is that of drying out. Loss of water can dry out the electrodes or the membrane, leading to a runaway in overheating and current loss and damage to the membrane. On the other hand, if too much liquid water accumulates at an electrode, it can block the diffusion of gas into that electrode, preventing dissociation and slowing down the overall conversion to electricity. Drops in current density are often the symptoms of flooding. A balance is therefore needed, which takes care to achieve. (Larminie et al. 2003).

Voltage is higher with humidified flow than with unhumidified reactant streams. In test stations, external humidification is typically achieved by bubbling the reactants through a reservoir of water. If the temperature and flow rate are high enough, the warmed oxidant can vaporize the product water and carry it away as water vapor. If the oxidant pressure and flow rate are high enough, the liquid water is physically pushed out, although flow rates that are too high will dry out the membrane and anode. Proton exchange membrane requires water to swell and have suitable ionic conductivity. In the absence of sufficient hydration, the membrane is too dry and the ohmic drop across the membrane becomes large. At higher current densities, however, the water produced at the cathode can condense and form a thin liquid film that blocks oxygen transport to the cathode (Gomez, 2001).

The different water movements are shown in Figure 2.4. Fortunately, all these water movements are predictable and controllable. Starting from the top of Figure 2.4, the water production and the water drag are both directly proportional to the current. During the operation of the cell the H^+ ions moving from the anode to the cathode pull water molecules with them. This process is sometimes called electro-osmotic drag. Typically, between one and five water molecules are dragged for each proton (Zawodzinski et al., 1993 and Ren and Gottesfeld, 2001). The water evaporation can be predicted with care theoretically considering the partial pressure of water vapor at certain temperature. The back diffusion of water from cathode to anode depends on the thickness of the electrolyte membrane and the relative humidity of each side. Finally, if external humidification of the reactant gases is used prior to entry into the fuel cell, this is a process that can be controlled.

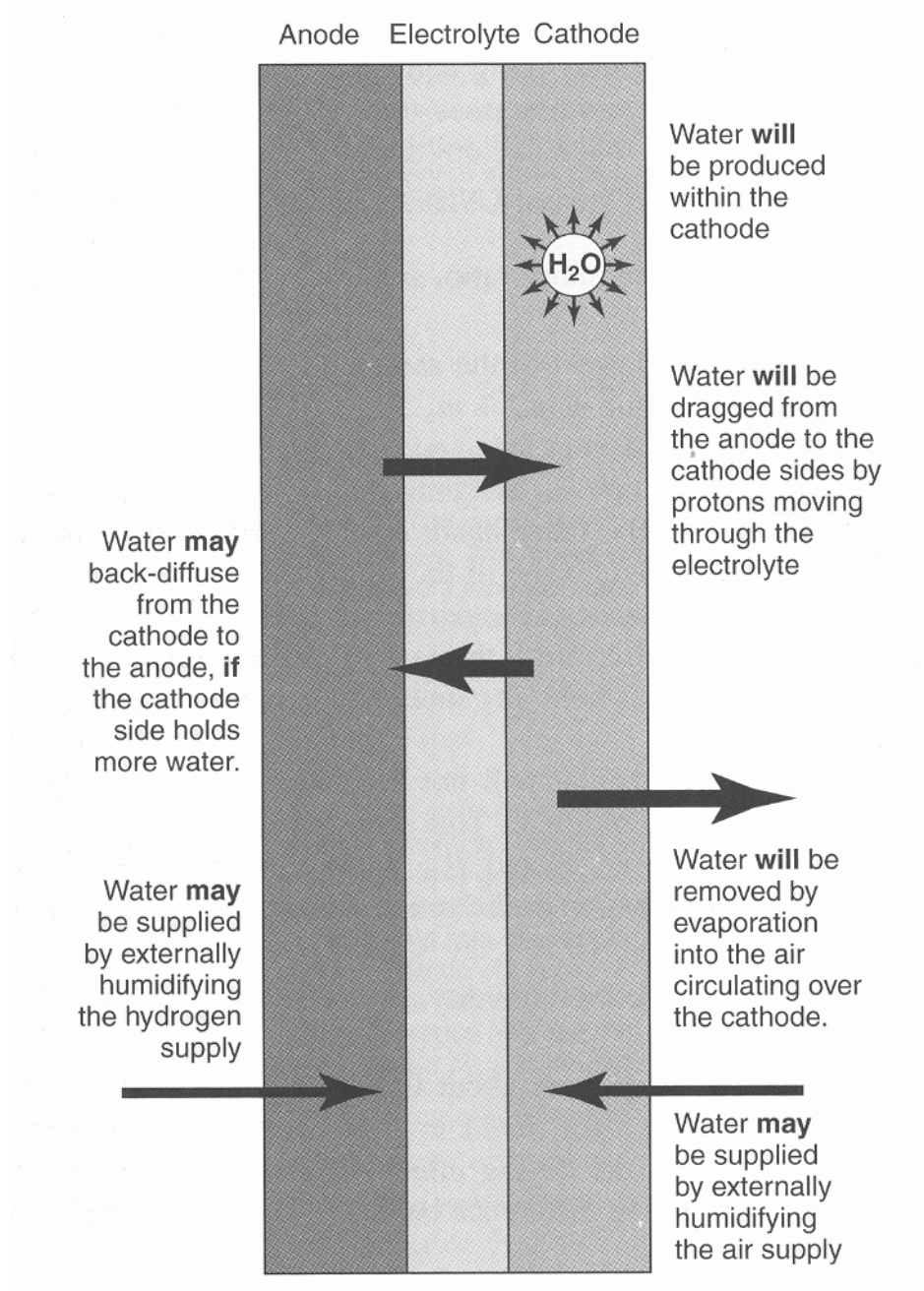


Figure 2.4 The different water movements to, within and from the electrolyte of a PEMFC

2.7 Thermodynamics of PEMFCs

In a fuel cell, it is the change in Gibbs free energy of formation, ΔG_f , that

gives us the energy released. This change is the difference between the Gibbs free energy of the products and the Gibbs free energy of the inputs or reactants.

$$\Delta G_f = G_f \text{ of products} - G_f \text{ of reactants} \quad [2.1]$$

Consider the basic reaction for the hydrogen/oxygen fuel cell.



The product is one mole of H₂O and the reactants are one mole of H₂ and a half a mole of O₂. Thus we have

$$\Delta G_f = (G_f)_{\text{H}_2\text{O}} - (G_f)_{\text{H}_2} - (G_f)_{\text{O}_2} \quad [2.3]$$

If there were no losses in the fuel cell, or as we should more properly say, if the process was reversible, then all Gibbs free energy would be converted into electrical energy. We will use this to find the reversible open current voltage (OCV) of a fuel cell.

For the hydrogen fuel cell, two electrons pass round the external circuit for each water molecule produced and each molecule of hydrogen used. So for one mole of hydrogen used, 2N electrons pass round the external circuit where N is Avagadro's number. If e⁻ is the charge on one electron, then the charge that flows is

$$-2 N e^- = -2 F \quad [2.4]$$

F being the faraday constant in coulombs, or the charge on one mole of electrons.

If E is the voltage of the fuel cell, then the electrical work done moving this charge round the circuit is

$$\text{Electrical work done} = \text{charge} \times \text{voltage} = -2 F E \text{ (joules)} \quad [2.5]$$

If the system is reversible (or has no losses), then this electrical work done will be equal to the Gibbs free energy released ΔG_f . So

$$\Delta G_f = -2 F E \quad [2.6]$$

Thus

$$E = \frac{-\Delta G_f}{2F} \quad [2.7]$$

This fundamental equation gives the electromotive force (EMF) or reversible open circuit voltage of the hydrogen fuel cell.

Using thermodynamic arguments, it can be shown that in the case of the hydrogen fuel cell reaction

$$\Delta G_f = \Delta G_f^0 - RT \ln \left(\frac{a_{H_2} \cdot a_{O_2}^{1/2}}{a_{H_2O}} \right) \quad [2.8]$$

We can see that if the activity of the reactants increases, ΔG_f becomes more negative, that is, more energy is released. On the other hand, if the activity of the product increases, ΔG_f increases, so becomes less negative and less energy is released. To see how this equation affects voltage, we can substitute it into Equation 2.7 and obtain and with a final organization we get

$$E = E^0 + \frac{RT}{2F} \ln \left(\frac{a_{H_2} \cdot a_{O_2}^{1/2}}{a_{H_2O}} \right) \quad [2.9]$$

where E^0 is the EMF at standard pressure. The equation shows precisely how raising the activity of the reactants increases the voltage. Equation 2.3 which gives an EMF in terms of product and/or reactant activity called Nernst equation. The EMF calculated from such equations is known as the Nernst voltage and is the reversible cell voltage that would exist at a given temperature and pressure.

2.8 Fuel cell irreversibilities and causes of voltage loss

The characteristic shape of the voltage-current density graphs of Figure 2.5

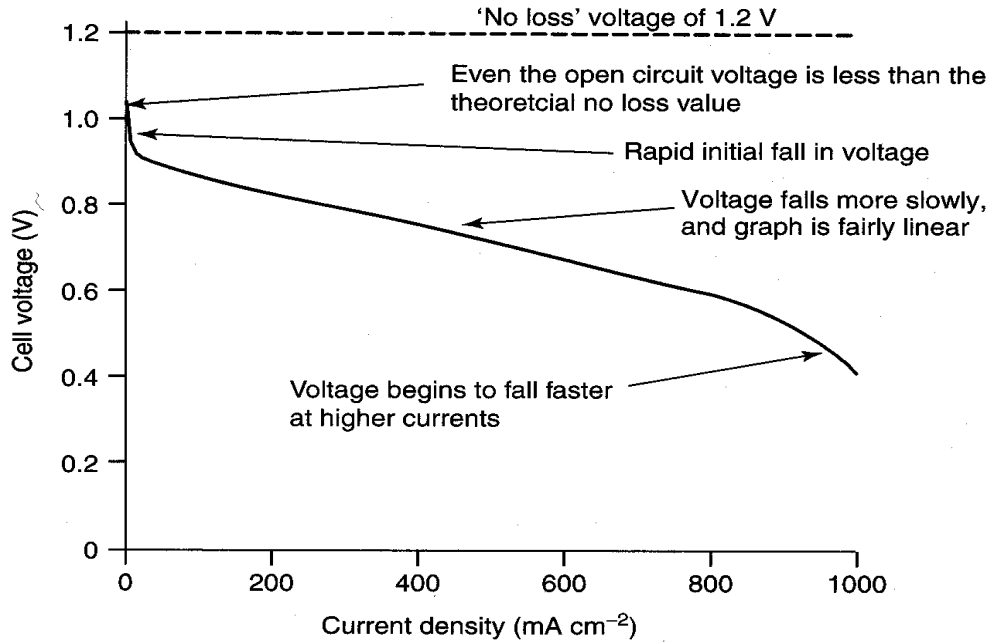


Figure 2.5.a Graph showing the voltage for a typical low temperature, air pressure fuel cell.

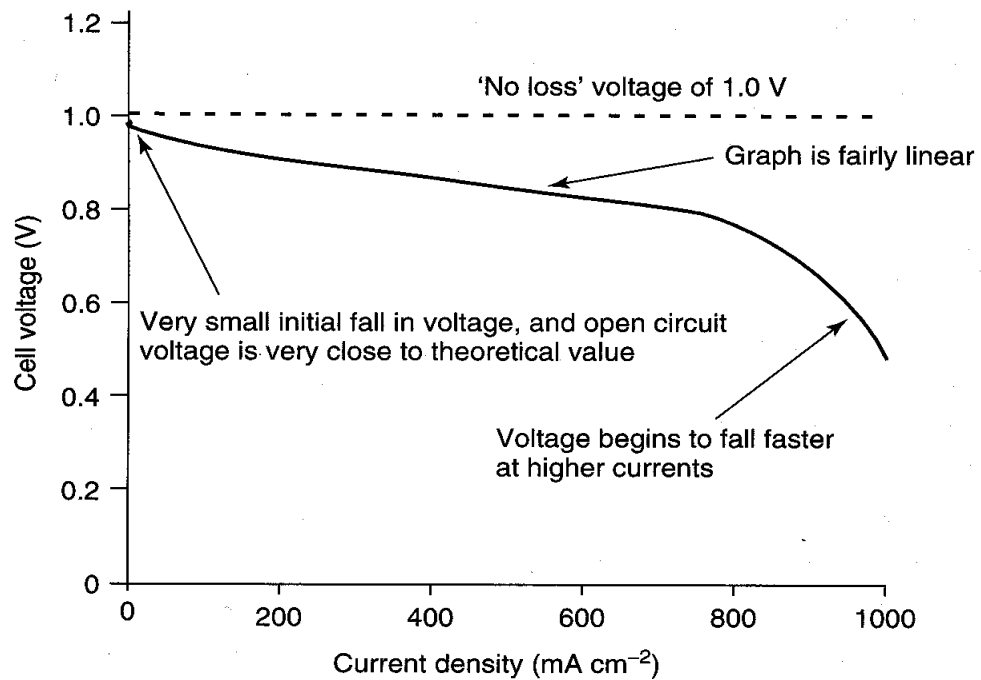


Figure 2.5.b Graph showing the voltage for a typical air pressure fuel cell operating at about 800 °C.

result from four major irreversibilities. This will be outlined very briefly here and then considered in more detail in the sections that follow.

Activation losses. These are caused by the slowness of the reactions taking place on the surface of the electrodes. A proportion of the voltage generated is lost in driving the chemical reaction that transfers the electrons to or from the electrode. This voltage drop is highly non-linear.

Fuel crossover and internal currents. This energy loss results from the waste of fuel passing through the electrolyte, and, to a lesser extent, from electron conduction through the electrolyte. The electrolyte should only transport ions through the cell. However, a certain amount of fuel diffusion and electron flow will always be possible and it does have a marked effect on the OCV of low-temperature cells.

Ohmic losses. This voltage drop is the straightforward resistance to the flow of electrons through the material of the electrodes and the various interconnections, as well as the resistance to the flow of ions through the electrolyte. This voltage drop is essentially proportional to current density, linear, and so is called *ohmic losses*, or sometimes as resistive losses.

Mass transport or concentration losses. These result from the change in concentration of the reactants at the surface of the electrodes as the fuel is used. Because the reduction in concentration is the result of a failure to transport sufficient reactant to the electrode surface, this type of loss is also often called mass transport loss. This type of loss has a third name Nernstian. This is because of its connections

with concentration, and the effects of concentration are modelled by the Nernst equation.

These four categories of irreversibility are considered one by one in the sections that follow.

2.8.1 Activation losses

2.8.1.1 The Tafel equation

As a result of experiments, rather than theoretical considerations, Tafel observed and reported in 1905 that the overvoltage at the surface of an electrode followed a similar pattern in a great variety of electrochemical reactions. This general pattern is shown in Figure 2.6. It shows that if a graph of overvoltage against log of current density is plotted, then, for most values of overvoltage, the graph approximates to a straight line. Such plots of overvoltage against log of current density are known as Tafel Plots. The diagram shows two typical plots.

For most values of overvoltage its value is given by the equation

$$\Delta V_{\text{act}} = a \cdot \log\left(\frac{i}{i_0}\right) \quad [2.10]$$

This equation is known as the Tafel equation. It can be expressed in many forms. One simple variation is to use natural logarithms instead of base 10. This gives

$$\Delta V_{\text{act}} = A \cdot \ln\left(\frac{i}{i_0}\right) \quad [2.11]$$

The constant A is higher for an electrochemical reaction that is slow. The constant i_0 is higher if the reaction is faster. The current density i_0 can be considered as the current density at which the overvoltage begins to move from zero. It is important to remember that the Tafel equation only holds true when $i > i_0$. This current density i_0 is usually called the exchange current density.

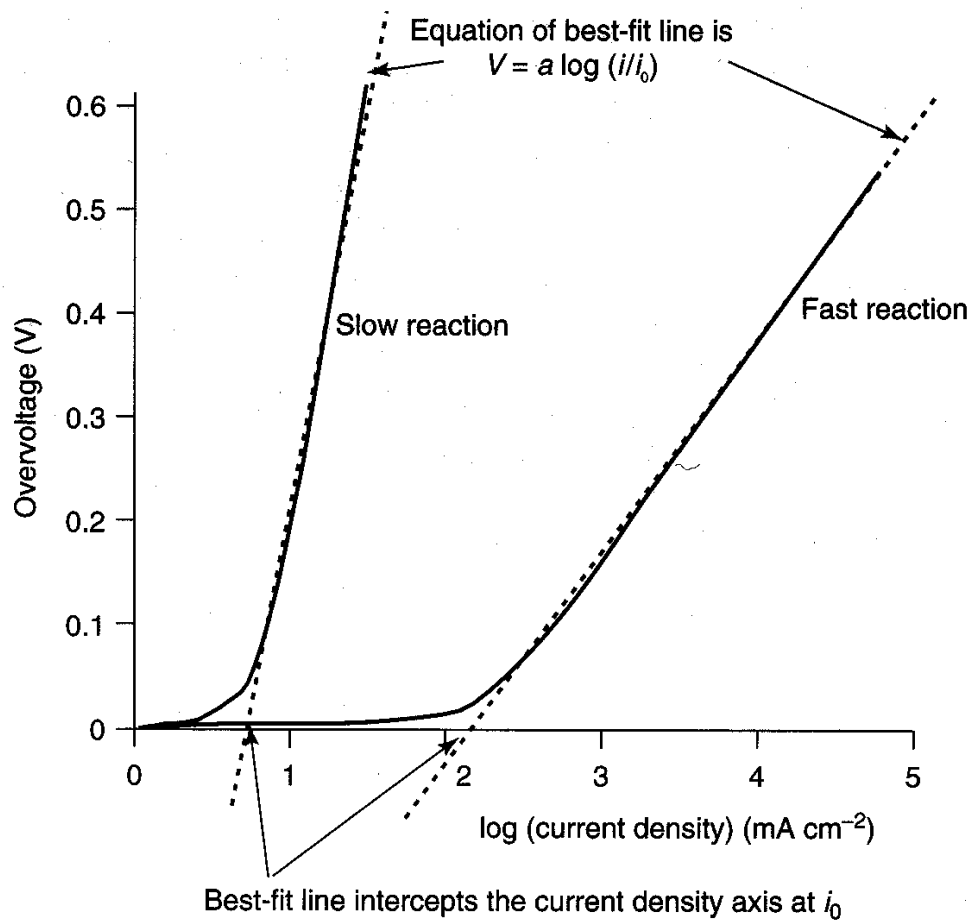


Figure 2.6 Tafel plots for slow and fast electrochemical reactions

Although the Tafel equation was originally deduced from experimental results, it also has a theoretical basis. It can be shown (Larminie et.al, 2003) that for a hydrogen fuel cell with two electrons transferred per mole, the constant A in Equation 2.11 above is given by

$$A = \frac{RT}{2\alpha F} \quad [2.12]$$

The constant α is called the charge transfer coefficient and is the proportion of the electrical energy applied that is harnessed in changing the rate of an electrochemical reaction. Its value depends on the reaction involved and the material the electrode is made from, but it must be in the range 0 to 1.0. For the hydrogen electrode, its value is about 0.5 for a great variety of electrode materials (Larminie et.al., 2003). At the oxygen electrode the charge transfer coefficient shows more variation, but is still between about 0.1 and 0.5 in most circumstances. In short, experimenting with different materials to get the best possible value for A will make little impact.

The appearance of T in Equation 2.12 might give the impression that raising the temperature increases the overvoltage. In fact this is very rarely the case, as the effect of increases in i_0 with temperature far outweigh any increase in A . Indeed, we shall see that the key to making the activation overvoltage as low as possible is this i_0 which can vary by several orders of magnitude. Furthermore, it is affected by several parameters other than the material used for the electrode.

The current density i_0 is called the exchange current density, and it can be visualized as follows. The reaction at the oxygen electrode of a proton exchange membrane (PEM) fuel cell is



At zero current density, we might suppose that there was no activity at the electrode and that this reaction does not take place. In fact this is not so; the reaction is taking place all the time, but the reverse reaction is also taking place at the same rate. Thus, there is a continual backwards and forwards flow of electrons from and to the electrolyte. This current density is i_0 , the exchange current density. It is self-evident that if this current density is high, then the surface of the electrode is more active and a current in one particular direction is more likely to flow. We are simply shifting in one particular direction something already going on, rather than starting something new.

This exchange current density i_0 is crucial in controlling the performance of a fuel cell electrode. It is vital to make its value as high as possible.

We should note that it is possible to change around the Tafel Equation 2.11 so that it gives the current, rather than the voltage. This is done by rearranging, and converting from the logarithmic to the exponential form. It is thus possible to show that Equation 2.11, with 2.12, can be rearranged to give

$$i = i_0 \exp\left(\frac{2\alpha F \Delta V_{\text{act}}}{RT}\right) \quad [2.14]$$

The equation is called the *Butler-Vollmer equation* and is quite often used as an equivalent alternative to the Tafel equation.

Imagine a fuel cell that has no losses at all except for this activation overvoltage on one electrode. Its voltage would then be given by the equation

$$V = E - A \ln\left(\frac{i}{i_0}\right) \quad [2.15]$$

where E is the reversible OCV. If we plot graphs of this equation using values

of i_0 of 0.01, 1.0, and 100 mA cm⁻², using a typical value for A of 0.06 V, we get the curves shown in Figure 2.7.

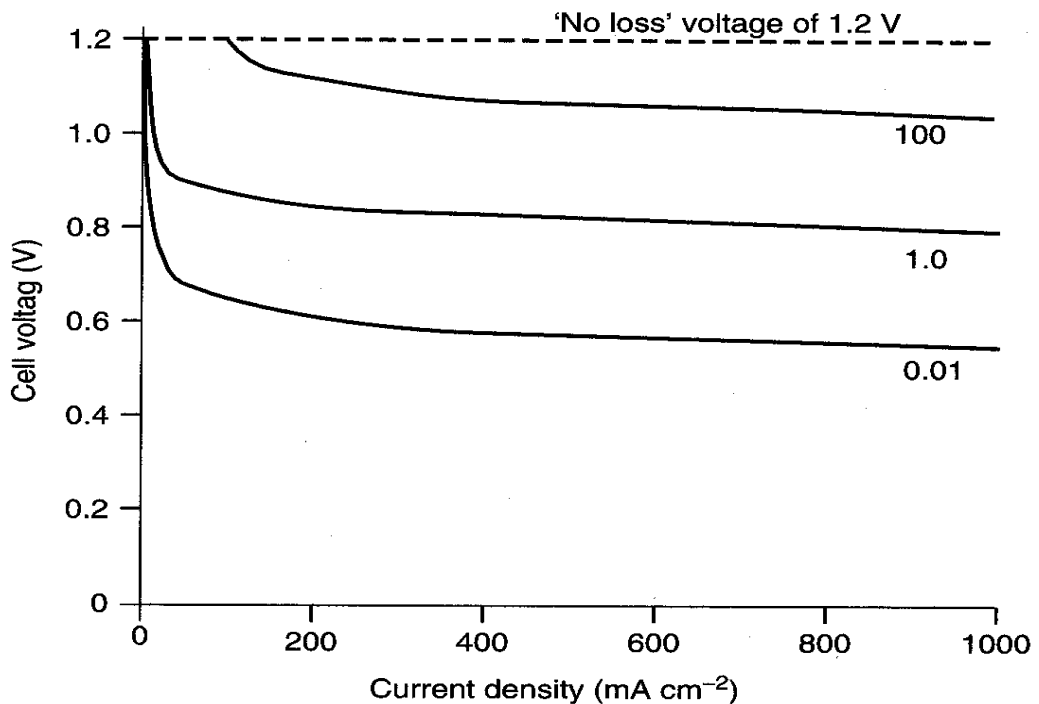


Figure 2.7 Graphs of cell voltage against current density, assuming all losses due only to the activation overvoltage at one electrode, for exchange current density i_0 values of 0.01, 1.0 and 100 mA cm⁻²

The importance of i_0 can be clearly seen. The effect, for most values of current density, is to reduce the cell voltage by a fairly fixed amount, as we could predict from the Tafel equation. The smaller the i_0 the greater is this voltage drop. Note that when i_0 is 100 mA cm⁻², there is no voltage drop until the current density i is greater than 100 mA cm⁻².

It is possible to measure this overvoltage at each electrode, either using reference electrodes within a working fuel cell or using half-cells. Table 2.1 below gives the values of i_0 for the hydrogen electrode at 25°C, for various metals. The measurements are for flat smooth electrodes.

Table 2.1 i_0 for the hydrogen electrode for various metals, for an acid electrolyte. (Larminie et.al., 2003)

| Metal | i_0 (A cm ⁻²) |
|-------|-----------------------------|
| Pb | 2.5×10^{-13} |
| Zn | 3×10^{-11} |
| Ag | 4×10^{-7} |
| Ni | 6×10^{-6} |
| Pt | 5×10^{-4} |
| Pd | 4×10^{-3} |

The most striking thing about these figures is their great variation, indicating a strong catalytic effect. The figures for the oxygen electrode also vary greatly and are generally lower by a factor of about 10^5 , that is, they are much smaller (Appleby and Foulkes, 1993). This would give a figure that is about 10^{-8} A cm⁻², even using Pt catalyst, far worse than even the lowest curve on Figure 2.7. However, the value of i_0 for a real fuel cell electrode is much higher than the figures in Table 2.1, because of the roughness of the electrode. This makes the real surface area many times bigger, typically at least 10^3 times larger than the nominal length x width.

We have noted that i_0 at the oxygen electrode (the cathode) is much smaller than that at the hydrogen anode, sometimes 10^5 times smaller. Indeed, it is generally reckoned that the overvoltage at the anode is negligible compared to that of the cathode, at least in the case of hydrogen fuel cells. For a low temperature, hydrogen-fed fuel cell running on air at ambient pressure, a typical value for i_0 would be about 0.1 mA cm⁻² at the cathode and about 200 mA cm⁻² at the anode.

2.8.1.2 Reducing the activation overvoltage

The exchange current density i_0 is the crucial factor in reducing the activation overvoltage. A crucial factor in improving fuel cell performance is, therefore, to increase the value of i_0 , especially at the cathode. This can be done in the following ways:

Raising the cell temperature. This fully explains the different shape of the voltage-current density graphs of low and high-temperature fuel cells illustrated in Figures 2.3.a and 2.3.b. For a low-temperature cell, i_0 at the cathode will be about 0.1 mA cm^{-2} , whereas for a typical 800°C cell, it will be about 10 mA cm^{-2} , a 100-fold improvement.

Using more effective catalysts. The effect of different metals in the electrode is shown clearly by the figures in Table 2.1.

Increasing the roughness of the electrodes. This increases the real surface area of each nominal 1 cm^2 , and this increases i_0 .

Increasing reactant concentration, for example, using pure O_2 instead of air. This works because the catalyst sites are more effectively occupied by reactants.

Increasing the pressure. This is also presumed to work by increasing catalyst site occupancy. (This also increases the reversible open circuit voltage, and so brings a double benefit.)

Increasing the value of i_0 has the effect of raising the cell voltage by a constant amount at most currents, and so mimics raising the open circuit voltage (OCV). (See Figure 2.7 above.) The last two points in the above list explain the discrepancy between theoretical OCV and actual OCV.

2.8.2 Fuel Crossover and internal currents

Although the electrolyte of a fuel cell would have been chosen for its ion conducting properties, it will always be able to support very small amounts of electron conduction. The situation is akin to minority carrier conduction in semiconductors. Probably more important in a practical fuel cell is that some fuel will diffuse from the anode through the electrolyte to the cathode. Here, because of the catalyst, it will react directly with the oxygen, producing no current from the cell. This small amount of wasted fuel that migrates through the electrolyte is known as fuel crossover.

These effects -fuel crossover and internal currents- are essentially equivalent. The crossing over of one hydrogen molecule from anode to cathode where it reacts, wasting two electrons amounts to exactly the same as two electrons crossing from anode to cathode internally, rather than as an external current. Furthermore, if the major loss in the cell is the transfer of electrons at the cathode interface, which is the case in hydrogen fuel cells, then the effect of both these phenomena on the cell voltage are also the same.

Although internal currents and fuel crossover are essentially equivalent, and the fuel crossover is probably more important, the effect of these two phenomena on the cell voltage is easier to understand if we just consider the internal current. We, as it were, assign the fuel crossover as equivalent to an internal current. This is done in the explanation that follows.

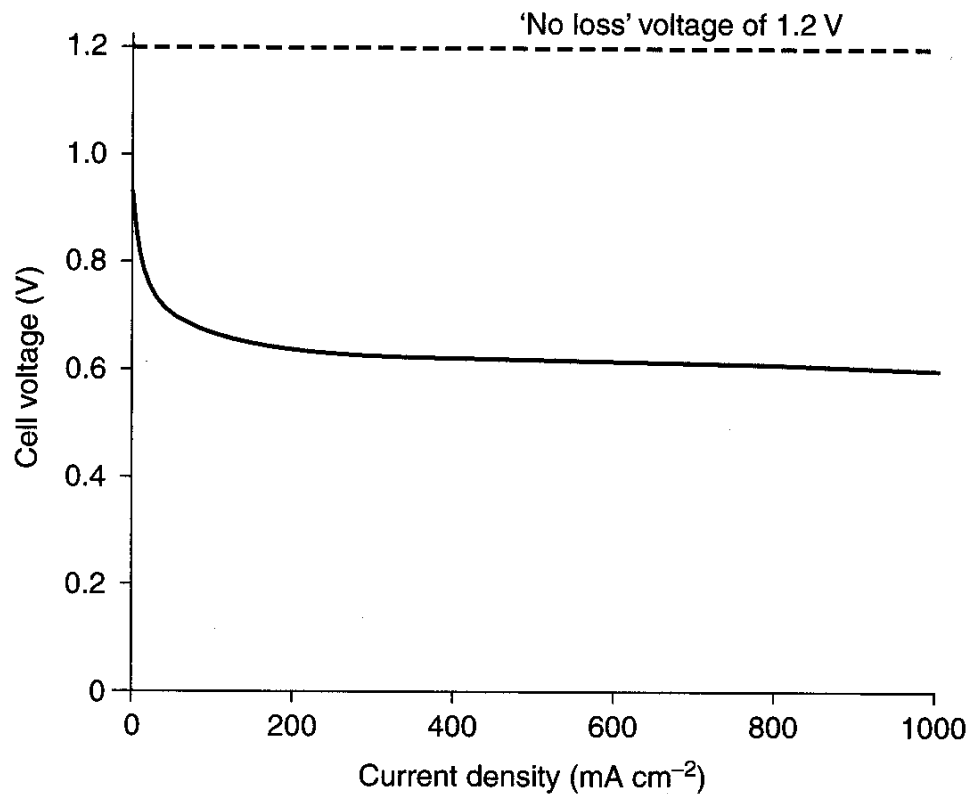


Figure 2.8 Graph showing the fuel cell voltage modeled using activation and fuel crossover/internal current losses only.

The flow of fuel and electrons will be small, typically the equivalent of only a few mA cm⁻². In terms of energy loss this irreversibility is not very important. However, in low-temperature cells it does cause a very noticeable voltage drop at open circuit. Users of fuel cells can readily accept that the working voltage of a cell will be less than the theoretical no loss reversible voltage. However, at open circuit, when no work is being done, surely it should be the same. With low-temperature cells, such as PEM cells, if operating on air at ambient pressure, the voltage will usually be at least 0.2 V less than the 1.2 V reversible voltage that might be expected.

If, as in the last section, we suppose that we have a fuel cell that only has losses caused by the activation overvoltage on the cathode, then the voltage will be as in Equation 2.15.

For the case in point, a PEM fuel cell using air, at normal pressure, at about 30°C, reasonable values for the constants in this equation are

$$E = 1.2\text{V} \quad A = 0.06\text{V} \quad \text{and} \quad i_0 = 0.04 \text{ mA cm}^{-2}$$

If we draw up a table of the values of V at low values of current density, we get the following values given in Table 2.2.

Now, because of the internal current density, the cell current density is not zero, even if the cell is open circuit. So, for example, if the internal current density is 1 mA cm^{-2} then the open circuit would be 0.97 V , over 0.2 V (or 20%) less than the theoretical OCV. This large deviation from the reversible voltage is caused by the very steep initial fall in voltage that we can see in the curves of Figure 2.5. The steepness of the curve also explains another observation about low-temperature fuel cells, which is that the OCV is highly variable. The graphs and Table 2.2 tell us that a small change in fuel crossover and/or internal current, caused, for example, by a change in humidity of the electrolyte, can cause a large change in OCV.

The equivalence of the fuel crossover and the internal currents on the open circuits is an approximation, but is quite a fair one in the case of hydrogen fuel cells where the cathode activation overvoltage dominates. However, the term mixed potential is often used to describe the situation that arises with fuel crossover.

If i_n is the value of this internal current density, then the equation for cell voltage that we have been using, Equation 2.15, can be refined to

$$V = E - A \ln\left(\frac{i + i_n}{i_0}\right) \quad [2.16]$$

Table 2.2 Cell voltages at low current densities (Larmnie et. al., 2003)

| Current density (mA cm ⁻²) | Voltage (volts) |
|--|-----------------|
| 0 | 1.2 |
| 0.25 | 1.05 |
| 0.5 | 1.01 |
| 1.0 | 0.97 |
| 2.0 | 0.92 |
| 3.0 | 0.90 |
| 4.0 | 0.88 |
| 5.0 | 0.87 |
| 6.0 | 0.86 |
| 7.0 | 0.85 |
| 8.0 | 0.84 |
| 9.0 | 0.83 |

2.8.3. Ohmic Losses

The losses due to the electrical resistance of the electrodes, and the resistance to the flow of ions in the electrolyte, are the simplest to understand and to model. The size of the voltage drop is simply proportional to the current, that is,

$$V = IR \quad [2.17]$$

In most fuel cells the resistance is mainly caused by the electrolyte, though the cell interconnects can also be important.

To be consistent with the other equations for voltage loss, the equation should be expressed in terms of current density. To do this we need to bring in the idea of the resistance corresponding to 1 cm² of the cell, for which we use the symbol r .

(This quantity is called the area-specific resistance or ASR.) The equation for the voltage drop then becomes

$$\Delta V_{\text{ohm}} = ir \quad [2.18]$$

where i is, as usual, the current density. If i is given in mA cm^{-2} , then the area-specific resistance, r , should be given in $\text{k}\Omega\text{cm}^2$.

Three ways of reducing the internal resistance of the cell are as follows:

- The use of electrodes with the highest possible conductivity.
- Good design and use of appropriate materials for the current collector plates and cell interconnects.
- Making the electrolyte as thin as possible. However, this is often difficult, as the electrolyte sometimes needs to be fairly thick as it is the support onto which the electrodes are built, or it needs to be wide enough to allow a circulating flow of electrolyte. In any case, it must certainly be thick enough to prevent any shorting of one electrode to another through the electrolyte, which implies a certain level of physical robustness.

2.8.4 Mass transport or concentration losses

If the oxygen at the cathode of a fuel cell is supplied in the form of air, then it is self evident that during fuel cell operation there will be a slight reduction in the concentration of the oxygen in the region of the electrode, as the oxygen is extracted. The extent of this change in concentration will depend on the current being taken from the fuel cell, and on physical factors relating to how well the air

around the cathode can circulate, and how quickly the oxygen can be replenished. This change in concentration will cause a reduction in the partial pressure of the oxygen.

Similarly, if the anode of a fuel cell is supplied with hydrogen, then there will be a slight drop in pressure if the hydrogen is consumed as a result of a current being drawn from the cell. This reduction in pressure results from the fact that there will be a flow of hydrogen down the supply ducts and tubes, and this flow will result in a pressure drop due to their fluid resistance. This reduction in pressure will depend on the electric current from the cell (and hence H₂ consumption) and the physical characteristics of the hydrogen supply system.

In both cases, the reduction in gas pressure will result in a reduction in voltage. However, it is generally agreed among fuel cell researchers that there is no analytical solution to the problem of modeling the changes in voltage that works satisfactorily in all cases (Kim et al., 1995). One approach that does yield an equation that has some value and use is to see the effect of this reduction in pressure (or partial pressure) by revisiting Equation 2.9; Nernst equation. Assuming reactant gases and vapor produced behaves as an ideal gas and if all the pressures are given in bar Equation 2.9 will become

$$E = E^0 + \frac{RT}{2F} \ln \left(\frac{P_{H_2} \cdot (P_{O_2})^{\frac{1}{2}}}{P_{H_2O}} \right) \quad [2.19]$$

If we isolate the pressure of hydrogen term in Equation 2.19 we have:

$$E = E^0 + \frac{RT}{2F} \ln \left(\frac{(P_{O_2})^{\frac{1}{2}}}{P_{H_2O}} \right) + \frac{RT}{2F} \ln(P_{H_2}) \quad [2.20]$$

So if the hydrogen partial pressure changes from P_1 to P_2 bar, with P_{O_2} and P_{H_2O} unchanged then the voltage will change by;

$$\Delta V = \frac{RT}{2F} \ln \left(\frac{P_2}{P_1} \right) \quad [2.21]$$

This gives the change in OCV caused by a change in pressure of the reactants. Now, the change in pressure caused by the use of the fuel gas can be estimated as follows. We postulate a limiting current density i_1 at which the fuel is used up at a rate equal to its maximum supply speed. The current density cannot rise above this value, because the fuel gas cannot be supplied at a greater rate. At this current density the pressure would have just reached zero. If P_1 is the pressure when the current density is zero, and we assume that the pressure falls linearly down to zero at the current density i_1 , then the pressure P_2 at any current density i is given by the formula

$$P_2 = P_1 \left(1 - \frac{i}{i_1} \right) \quad [2.22]$$

If we substitute this into Equation 2.22 (given above) and write in terms of a voltage drop, we obtain

$$\Delta V = \frac{RT}{2F} \ln \left(1 - \frac{i}{i_1} \right) \quad [2.23]$$

This gives us the voltage change due to the mass transport losses.

Now the term that in this case is $\frac{RT}{2F}$ will be different for different reactants,

as should be evident from Equation 2.19. For example, for oxygen it will be $\frac{RT}{4F}$.

In general, we may say that the concentration or mass transport losses are given by the equation

$$\Delta V_{\text{trans}} = -B \ln \left(1 - \frac{i}{i_1} \right) \quad [2.24]$$

where B is a constant that depends on the fuel cell and its operating state. For example, if B is set to 0.05 V and i_1 to 1000 mA cm⁻², then quite a good fit is made to curves such as those of Figures 2.3.a and b. However, this theoretical approach has many weaknesses, especially in the case of fuel cells supplied with air rather than pure oxygen which are the vast majority. There are also problems with lower-temperature cells, and those supplied with hydrogen mixed with other gases such as carbon dioxide for the fuel. No account is taken for the production and removal of reaction products, such as water, and neither is any account taken of the build-up of nitrogen in air systems.

Another approach that has no claim for a theoretical basis, but is entirely empirical, has become more favored lately, and yields an equation that fits the results very well (Kim et al., 1995 and Laurencelle et al., 2001). This approach uses Equation 2.25 below because it gives a very good fit to the results, provided the constants m and n are chosen properly.

$$\Delta V_{\text{trans}} = m \exp (ni) \quad [2.25]$$

The value of m will typically be about 3 x 10⁻⁵ V, and n about 8 x 10⁻³ cm² mA⁻¹. Although the Equations 2.24 and 2.25 look very different, if the constants are chosen carefully the results can be quite similar. However, Equation 2.25 can be used to give a better fit to measured results and appears to be quite widely used in the fuel cell community.

The mass transport or concentration overvoltage is particularly important in cases where the hydrogen is supplied from some kind of reformer, as there might be a difficulty in increasing the rate of supply of hydrogen quickly to respond to demand. Another important case is at the air cathode, if the air supply is not well circulated. A particular problem is that the nitrogen that is left behind after the oxygen is consumed can cause a mass transport problem at high currents it effectively blocks the oxygen supply. In proton exchange membrane fuel cells (PEMFCs), the removal of water can also be a cause of mass transport or concentration overvoltage.

2.9. Efficiency of a fuel cell

The efficiency of a fuel cell is usually defined as

$$\frac{\text{electrical energy produced per mole of fuel}}{-\Delta H_f} \quad [2.26]$$

where ΔH_f is the enthalpy of formation. However, this is not without its ambiguities, as there are two different values we can use for ΔH_f . For the burning of hydrogen where the product is steam $\Delta H_f = -241.83 \text{ kJ mol}^{-1}$ (LHV). On the other hand, if the product water is condensed back to liquid then $\Delta H_f = -285.84 \text{ kJ mol}^{-1}$ (HHV).

The maximum electrical energy available is equal to the change in Gibbs free energy, so

$$\text{Maximum energy possible} = \frac{\Delta G_f}{\Delta H_f} \times 100\% \quad [2.27]$$

The operating voltage of a fuel cell can be related to its efficiency. This can be shown by adapting Equation 2.7. If all the energy from the hydrogen fuel, its enthalpy of formation, were transformed into electrical energy, then the EMF would be given by

$$E = \frac{-\Delta H_f}{2F} \quad [2.28]$$

=1.48 V if using the HHV

or = 1.25 V if using the LHV

These are the voltages that would be obtained from a 100% efficient system, with reference to the HHV or LHV. The actual efficiency of the fuel cell is then the actual voltage divided by these values, or

$$\text{Cell efficiency} = \frac{V_c}{1.48} 100\% \text{ (With reference to HHV)} \quad [2.29]$$

CHAPTER 3

EXPERIMENTAL

Experimental work was conducted in three phases. The first phase was to build a test station to perform the performance tests of fuel cells to be constructed. Second phase was to construct fuel cells which were different in structure and materials used. Fuel cell which showed the best performance was chosen for the third phase of the experimental work. In the third phase a parametric study was performed on the fuel cell chosen in the second phase. Details of these phases of the experimental work will be explained in the following sections of this chapter.

3.1. Building test station

The test station built was capable of controlling the flow rate and humidification temperature of reactant gases, fuel cell temperature and electrical load applied to the fuel cell. For the purpose of controlling the flow rate of reactant gases two (Aalborg GFC171) gas mass flow controllers were used. Humidification of the gases was performed by bubbling them through washing bottles containing distilled water. Bottles were placed in a temperature controlled hot water bath (Thelco Model 83).

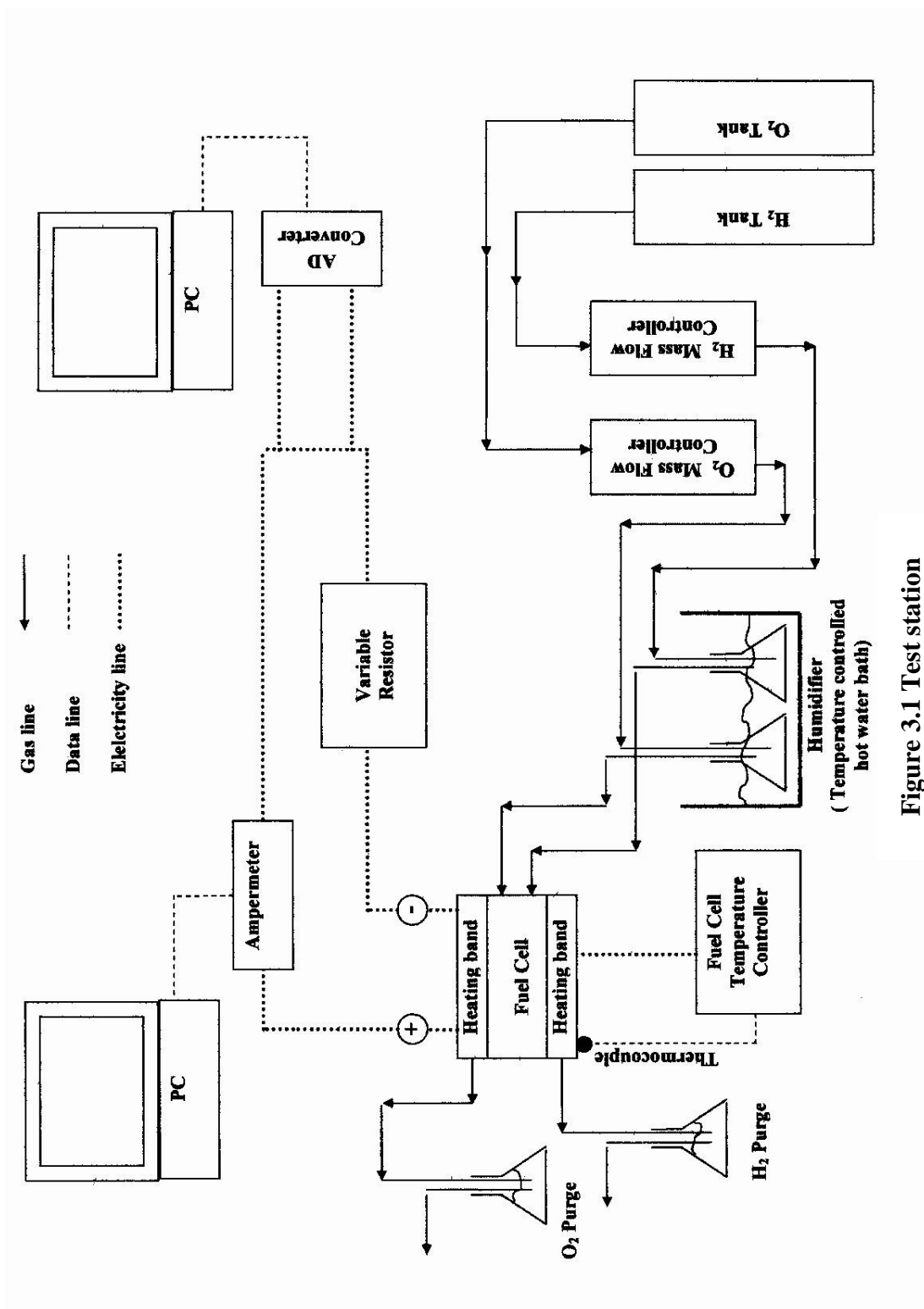


Figure 3.1 Test station

All gas lines were 0.6 cm diameter copper tubing. Gas lines carrying the reactants were insulated to prevent the condensation of water within the lines.

Unreacted gases were purged from the fuel cell to the atmosphere by bubbling them through cold water. A very thin thermocouple was inserted to the back of one of the graphite plates used within the fuel cell which was then linked to the temperature controller (Industrial Electronic Equipments, Model GE XDD1DC096). Heating of the fuel cell was achieved by using a heating band wrapped around the casing of the fuel cell which was controlled by the temperature controller. A variable resistor was used to alter the electrical load over the fuel cell. An ampermeter (Breyden BM 850) and an AD converter card (Advantech PCL-711) were connected to the fuel cell properly to complete the circuit for the purpose of measuring current and voltage produced by the fuel cell. Data from the ampermeter was logged through the RS-232 port of a PC using the software came with the ampermeter. Voltage was logged by another PC through the AD converter card using its own software. High purity hydrogen and oxygen gases were used as reactants. A representation of the test station built is given in Figure 3.1.

3.2. Construction of fuel cells

Five different fuel cells, namely EAE1, AOY001, AOY001, AOY003 and AOY004 were constructed. They were different in structure, size and materials used. The aim to construct different fuel cells was to understand their structure and to find proper materials for construction. Also different methods were used to manufacture the membrane electrode assemblies and machine the gas distribution channels on the graphite plates of the fuel cells. A representative figure showing the parts

of the fuel cells constructed is given in Figure 3.2.

3.2.1. Materials used to construct the fuel cells

In the following sections materials are classified according to where they were used.

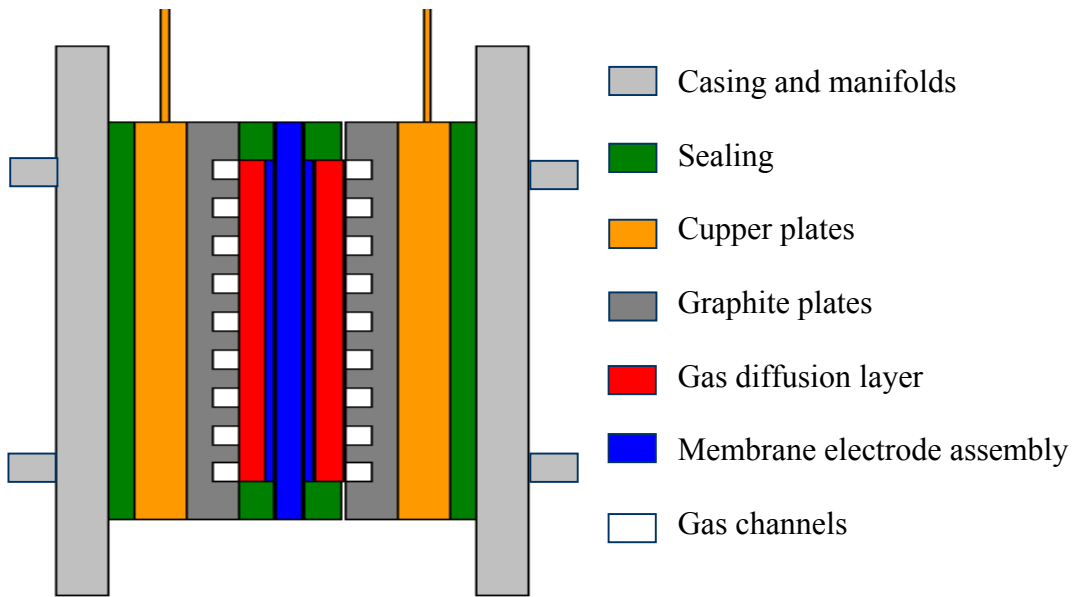


Figure 3.2 General structure of the PEMFCs constructed

3.2.1.1. Casing

Steel and “Kestamid” casing were used for fuel cells constructed. Kestamid is the commercial name of a polyamide which is strong as much as steel. However, its thermal conductivity is very low in comparison to steel.

3.2.1.2. Current collectors

3 mm thick copper plates were used as current collectors.

3.2.1.3. Gas distribution plates

Four different graphite plates were used as gas distribution plates. Suppliers and models of the graphite plates are:

- SGL Carbon BPP4 (SGL Carbon GmbH, Germany)
- Schunk FU427 (Schunk GmbH, Germany)
- Alfa Aesar Cat No: 10132 (Alfa Aesar, USA)
- Morgan AY1 (Morgan Inc., U.K.)

3.2.1.4. Gas diffusion layers

Gas diffusion layers were either manufactured or supplied by the producer company. To manufacture the gas diffusion layers rolling method was used (Han, 2000). Details of the rolling method are explained in the following section. SGL Carbon GDL 10 BA supplied by SGL Carbon GmbH, Germany was used as the backing layer of the manufactured gas diffusion layers. Charcoal activated pure (Merck 1.02183.1000), Teflon as the binder material and ammonium

bicarbonate as the pore making substance were used to form the coated layer over the backing layer. On the other hand, SGL Carbon GDL 10 BB gas diffusion layers were supplied by SGL Carbon GmbH, Germany in their finished form.

3.2.1.5 Membrane electrode assemblies (MEA)

As previously explained a MEA is obtained when both sides of a membrane is coated with a catalyst layer. MEAs used in the experiments were either manufactured or purchased. MEAs with different catalyst loadings were manufactured. To manufacture the MEAs rolling and spraying methods were used. Nafion 115 proton exchange membrane was used in all manufactured MEAs. Platinum on charcoal activated pure (10% Pt/C Alfa Aesar), and platinum on Vulcan XC-72 (20% Pt/C On Vulcan XC-72) were used as catalyst, Nafion solution (5% Nafion solution in lower aliphatic alcohols) as binder material in the catalyst layer coated over the membrane. On the other hand, finished MEAs were purchased from Ion Power Inc. USA. A V-i diagram sent by Ion-Power is given in Appendix C.

3.2.2. Methods used to manufacture gas diffusion layers and MEAs

3.2.2.1. Rolling method

Rolling method was previously developed for manufacturing alkaline fuel cell electrodes (Han, 1997). In the rolling method formation of the layers were achieved by rolling the materials over the carbon paper backing using a roller. First the gas diffusion layer was manufactured. Charcoal activated pure, Teflon, ammonium bicarbonate were mixed in N-Heptane and a suspension was obtained. After the suspension agent was filtered more liquid was removed by performing a series of kneading operation and workable dough was achieved. For the catalyst layer same steps were repeated replacing the charcoal activated pure by platinum on charcoal activated pure and adding Nafion solution. Then gas diffusion layer and active layer were cross rolled over the carbon paper backing which was cut to size. N-Heptane and ammonium bicarbonate were removed by keeping the final structure at 150 °C under vacuum for 1 hour. After thermal treatment sintering was achieved by pressing the electrode under slight pressure at 150 °C for 20 minutes. Finally Nafion membrane was placed between two electrodes and pressed for 3 minutes at 130 °C at 1000 psi.

3.2.2.2. Spraying method

Spraying method was used to manufacture the membrane electrode assemblies. Gas diffusion layers were not manufactured by spraying method. In spraying method layers were formed by spraying the catalyst layer material. First platinum on Vulcan XC-72 and Nafion solution were mixed in a 7:1 (v/v) ratio 2-propanol-water solution. Prepared suspension was sprayed over 0.5 mm

thick Teflon film which was cut to size with a spray gun (Head caliber 1:8). Before starting to spray, blank Teflon film was weighed. Then solvent was removed by thermal treatment at 100 °C until the solvent was visually disappeared and weighed to monitor the amount coated. This process was repeated until the desired catalyst loading is achieved. Teflon films coated were kept under vacuum at 100 °C for 1 hour to remove remaining solvent. Nafion membrane was boiled in H₂O₂ for half an hour to remove any organic substance that might be present on the surface and after that boiled in 0.5 M H₂SO₄ for 1 hour for the purpose of full protonation. Afterwards it was rinsed in distilled water many times. After rinsing the membrane it was quickly dried with a hot air gun at 50 °C to prevent any wrinkles that water may form on the membrane. Finally the membrane was placed between two coated Teflon films and pressed under 1250 psi for 3 minutes at 135 °C. Teflon films were peeled away from the membrane leaving the catalyst layer adhered to the membrane. Final structure was the catalyst coated membrane at both sides that was named as membrane electrode assembly.

3.2.3. Geometry of the gas distribution channels

Gas distribution channels are machined on the graphite gas distribution plates. These channels provide the transportation of reactant gases all over the gas diffusion layer and removal of produced water and condensate from the body of the cell. Two different geometries were used. First one is the serpentine flow geometry. In serpentine flow geometry a set of channels travel through the surface in a

parallel manner. Second one is the interdigitated flow geometry. In this geometry reactant gases flow through a set of parallel dead ended channels which has one opening from gas feed side and forced to diffuse to the gas diffusion layer. Unreacted gases pass to the other set of dead end channels which have one opening to the gas exit line. These two set of dead end parallel channels are placed like two combs collided each other. Both geometries were machined over the graphite plates at METU CAD-CAM (Computer Aided Design- Computer Aided Manufacturing) Center. Serpentine flow type geometry was machined with a “CNC Milling Machine” and interdigitated geometry was machined with a “CNC Erosion Driller”. Representative figures of the geometries used during the experiments are presented in Figures 3.3 and 3.4.

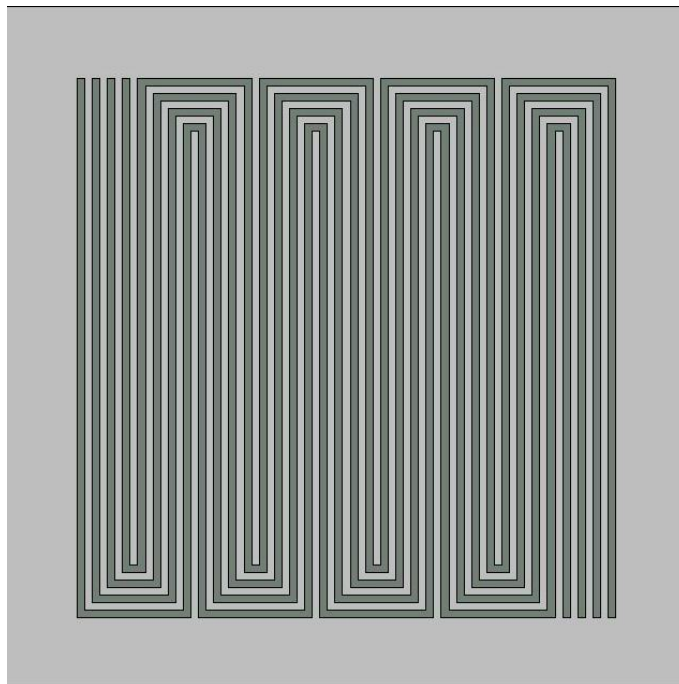


Figure 3.3 Serpentine flow patterns

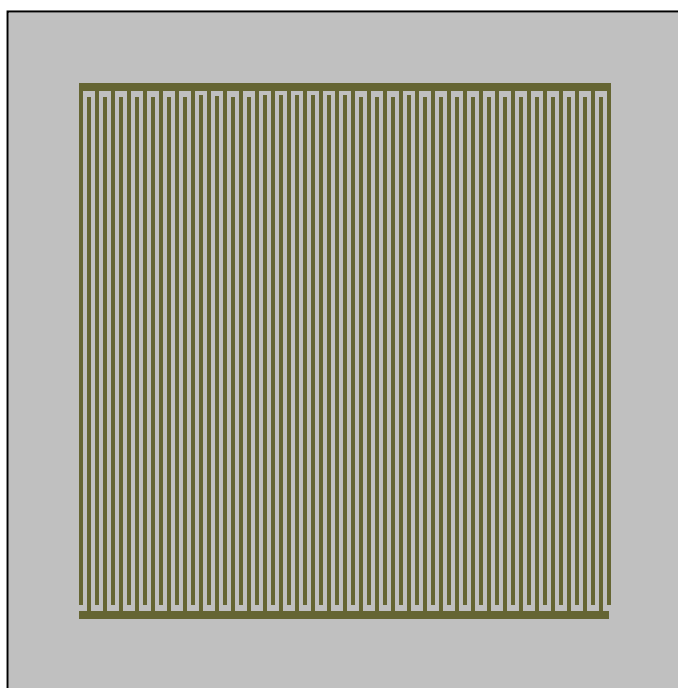


Figure 3.4 Interdigitated flow patterns

3.3 Experimental procedure

A standard procedure was applied to obtain the V-i diagrams. First, gas valves were opened and they were regulated to atmospheric pressure. Then, flow rate of the gases were set by previously calibrated gas mass flow controllers. Afterwards, water bath was heated to the desired humidification temperature. Finally, fuel cell

was heated to its operating temperature by setting the temperature controller. Here it should be noted that during the initial experiments which were performed to compare the performances of all PEMFCs, there were no gas mass flow controllers in the

laboratory. Instead, flow rates were set by at short circuit condition (full load) observing the gas bubbles exiting the PEMFC through the water containing bottles. Gas bubbles were minimized so that they were sufficient for the reaction to take place but not too much to cause any unpredictable effect.

After humidification and fuel cell temperatures reached the set points, PEMFC was operated between 0.6 V (for 30 minutes) and 0.4 V (for 30 minutes) and then for 1 minute at the open current voltage (OCV) conditions. To reach the pseudo steady state condition this cycle was repeated at least four times until no further significant increase was observed on the performance. Then voltage-current data were collected by varying the resistor to obtain V-i diagrams.

3.4. Scope of the work

According to the details given in section 3.2 about the construction of the fuel cells, a comparative table is formed to present the differences between the fuel cells constructed (Table 3.1).

Performance of the fuel cells constructed EAE1, AOY001, AOY001, AOY003 and AOY004 were compared according to their V-i diagrams obtained at $T_{Cell} = 25\text{ }^{\circ}\text{C}$ and $T_{Hum} = 25\text{ }^{\circ}\text{C}$. AOY001 which showed the best performance was chosen for further parametric studies. Effects of three different parameters on the performance of AOY001 were studied. These parameters were humidification temperature, excess flow rate condition of reactant gases, fuel cell temperature and H_2 to O_2 ratio.

The effect of humidification temperature of reactant gases at two different flow rates was investigated keeping the fuel cell temperature (50°C) and gas flow rates constant and changing the humidification temperature between 35 and 60 °C. Flow rates of H₂ and O₂ gases were 0.4 and 0.2 sLm (standard liters per minute) respectively for the excess amount condition, 0.1 and 0.05 sLm respectively for the other one.

The effect of fuel cell temperature was investigated at two different humidification conditions. Fuel cell temperature was changed between 30 and 60 °C while keeping the humidification temperature 10 °C more than the cell temperature in the first experiment and 5 °C less in the second case. Flow rates of H₂ and O₂ gases were 0.1 and 0.05 sLm respectively.

Table 3.1 Properties of the PEMFCs constructed

| Fuel cell / Electrode Area | Graphite plate | Flow field geometry / Channel width (mm) | Gas diffusion layer | MEA manufacturing method / Pt load / Nafion load (mg/ cm ²) | Membrane / Thickness (µm) |
|-----------------------------|-----------------|--|----------------------|---|---------------------------|
| EAE1/ 50 cm ² | Alfa-Aesar | Interdigitated / 0.5 | Rolling method | Rolling method / 0.56 / 0.4 | Nafion 115 / 125 |
| AOY001/ 50 cm ² | SGL Carbon BPP4 | Serpentine / 1 | SGL Carbon GDL 10 BB | Ion-Power proprietary/ 0.3 / 0.3 | Nafion 1100 EW / 25 |
| AOY002 / 50 cm ² | Morgan AY1 | Serpentine / 1 | SGL Carbon GDL 10 BB | Ion-Power proprietary / 0.3 / 0.3 | Nafion 1100 EW / 25 |
| AOY003 / 25 cm ² | Schunk FU427 | Interdigitated / 0.5 | SGL Carbon GDL 10 BB | Spraying method / 0.04 / 0.007 | Nafion 115 / 125 |

| | | | | | |
|--------------------------------|-----------------------|-------------------|----------------------------|----------------------------------|------------------------|
| AOY004 / 50 cm ² | SGL Carbon BPP4 | Serpentine / 1 | SGL Carbon GDL 10 BB | Spraying method / 0.29 / 0.45 | Nafion 115 / 125 |
|--------------------------------|-----------------------|-------------------|----------------------------|----------------------------------|------------------------|

The effect of O₂ to H₂ ratio was investigated by keeping the H₂ flow rate constant at 0.1 sLm and changing the O₂ flow rate between 0.05 and 0.1 sLm. Fuel cell temperature was kept constant at 60 °C while keeping humidification temperature at 70 °C.

Scope of the five different experiments are briefly tabulated in Table 3.2 .

Table 3.2 Scope of the experiments

| | T Cell (°C) | T Hum (°C) | H ₂ Flow Rate (sLm) | O ₂ Flow Rate (sLm) |
|-------|--------------|-------------|-----------------------------------|-----------------------------------|
| Run 1 | 50 | 35-60 | 0.4 | 0.2 |
| Run 2 | 50 | 35-60 | 0.1 | 0.05 |
| Run 3 | 30-60 | 40-70 | 0.1 | 0.05 |
| Run 4 | 30-60 | 25-55 | 0.1 | 0.05 |
| Run 5 | 60 | 70 | 0.1 | 0.05-0.1 |

CHAPTER 4

RESULTS AND DISCUSSION

It is important to be able to achieve the expected reversible potential and maximum efficiency of any given fuel cell. However, it is usually found that a cell does not operate reversibly, except perhaps at very low currents. The open circuit voltage of the fuel cell is often less than the reversible potential and as current is drawn from the fuel cell, the fuel cell voltage decreases. This is the general response of all fuel cells. The goal is to obtain high current density at high operating voltages.

In this study five different PEMFCs were constructed and their performances were compared through V-i diagrams obtained. The PEMFC which showed the best performance was chosen to observe the effects of different parameters on the performance of PEMFC.

4.1. Comparison of the constructed PEMFCs

EAE1, AOY001, AOY002, AOY003 and AOY004 were the PEMFCs constructed. The V-i diagrams of five fuel cells are shown in Figure 4.1. These data were obtained keeping the fuel cell and gas humidification temperature at 25 °C. A fuel cell's performance

can be evaluated by examining the characteristic V-i curve. What is desired from a PEMFC is to present a high open circuit voltage (OCV) and high current densities at voltages as high as possible. Comparing the current densities obtained at a constant voltage is a powerful tool to make a comparison provided that you have similar values of OCVs. Table 4.1 tabulates the OCVs and current densities at 0.5 V of the PEMFCs constructed.

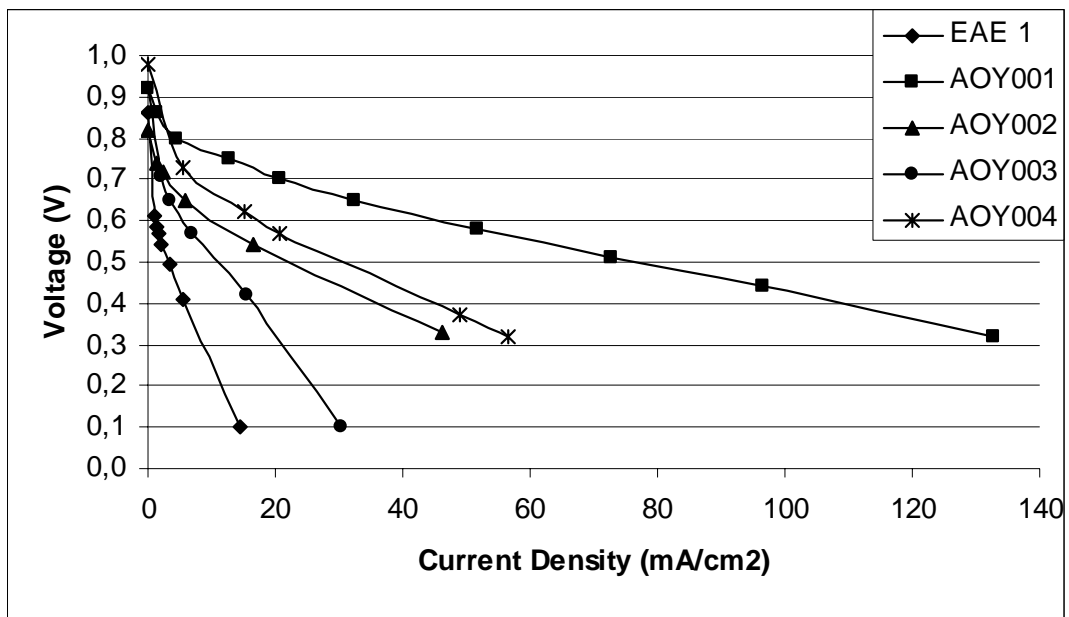


Figure 4.1 Performance comparison of the PEMFCs constructed
(T Cell = 25 °C, T Hum = 25 °C)

Table 4.1 OCVs and current densities of the constructed PE

| PEMFC | OCV (Volts) | Current density at 0.5 V (mA/cm ²) |
|--------|-------------|--|
| EAE1 | 0.86 | 3.3 |
| AOY001 | 0.92 | 77.5 |
| AOY002 | 0.82 | 23.1 |
| AOY003 | 0.92 | 11.9 |
| AOY004 | 0.98 | 31.7 |

It is clear that AOY001 delivered the highest current at the same voltage among all PEMFCs. It is also seen from Figure 4.1 that the curve for AOY001 represents better performance than other curves. Performance of a PEMFC depends on many factors, however, among them the two most important factors are the structure of the MEA combined with gas diffusion layers and the overall conductivity between the parts of the fuel cell. Operating conditions affect directly these two factors. Therefore, effect of operating conditions on the performance should be investigated independent from the structure of the PEMFC. Structure of the MEA strongly depends on the manufacturing method and materials used. The inter conductivity of the parts of the PEMFC depends on materials used and an effective assembly procedure. By inspecting the V-i curves it may be said that AOY001 has the optimum structure. Thus it was logical to study the effects of operating conditions on this PEMFC. In the next section, results of the effects of different operating conditions on the performance are presented.

4.2 Effect of operating conditions on the performance of the PEMFCs

Effects of humidification temperature of gases, cell temperature and oxygen to hydrogen ratio on the performance of the AOY001 were investigated. The results are compared through the V-i curves obtained at different conditions.

4.2.1 Effect of gas humidification temperature

Figure 4.2 shows the effect of gas humidification temperature with excess flow rate of reactants and Figure 4.3 shows the same effect under a flow condition in which the gases were fed with a 4 times lower flow rate. It can be seen that increasing gas humidification temperature has a significant positive effect on the performance under both conditions. In both graphs it can be seen that at 60 °C of gas humidification temperature the performances are at their highest values. When we compare two curves at 60 °C we see that at 0.5 V the one under excess flow rate delivered a current density of 103 mA/cm². On the other hand the other one with a lower flow rate of reactant gases delivered a current density of 127 mA/cm². Same behavior can be observed when other curves with same humidification temperatures are compared. It can be said that excess flow rate of reactant gases has a negative effect on the performance curve.

4.2.2 Effect of fuel cell temperature

Figure 4.4 shows the effect of cell temperature on the performance at a high level of humidification temperature where it is held 10 °C above cell temperature. Figure 4.5 shows the effect of cell temperature on the performance at a low level of humidification temperature where it is held 5 °C below cell temperature. In both figures the positive effect of increasing cell temperature can easily be seen.

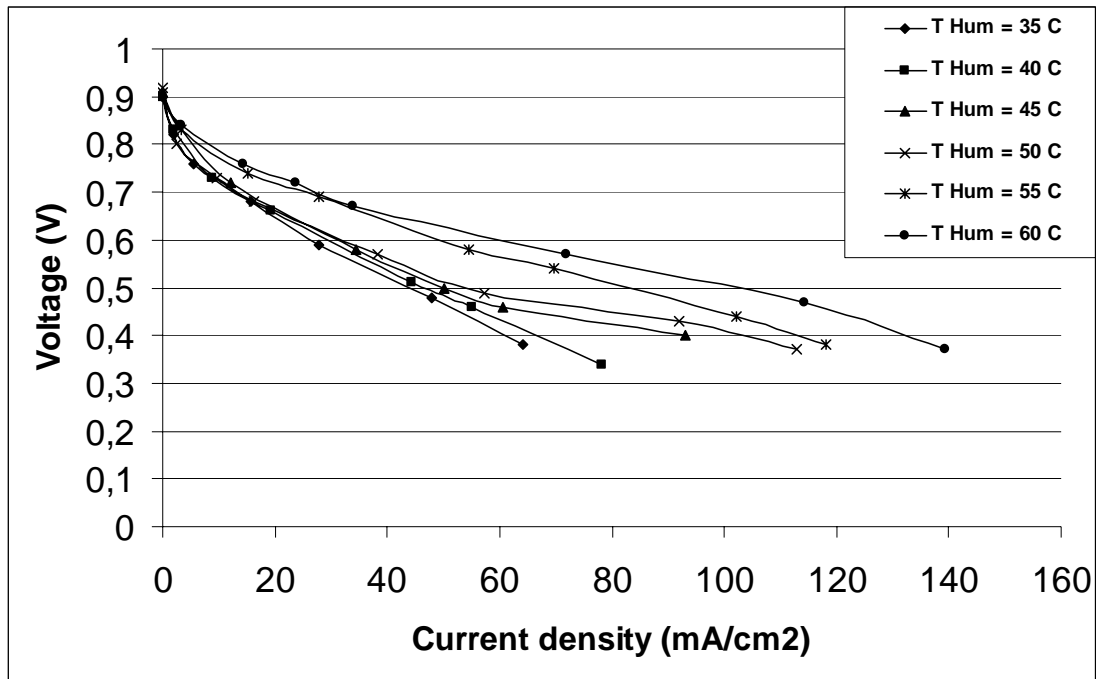


Figure 4.2 Effect of gas humidification temperature with excess flow rate of reactants. (T Cell = 50 °C; H₂: 0.4 sLm; O₂: 0.2 sLm).

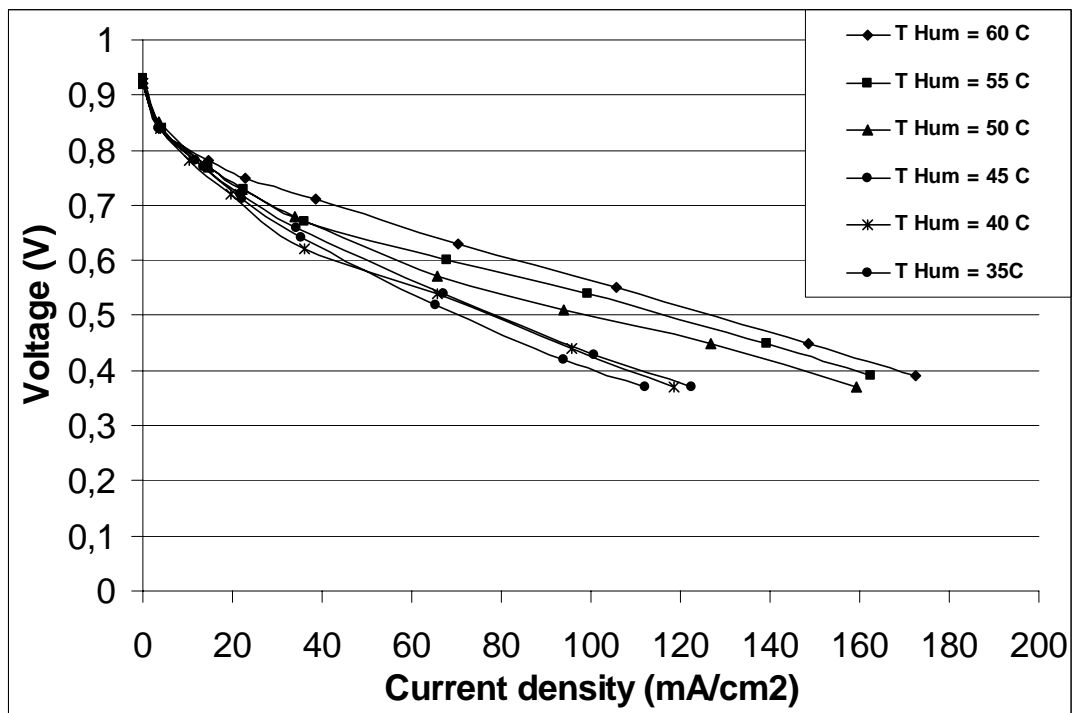


Figure 4.3 Effect of gas humidification temperature (T Cell = 50 °C; H₂: 0.1 sLm; O₂:0.05 sLm)

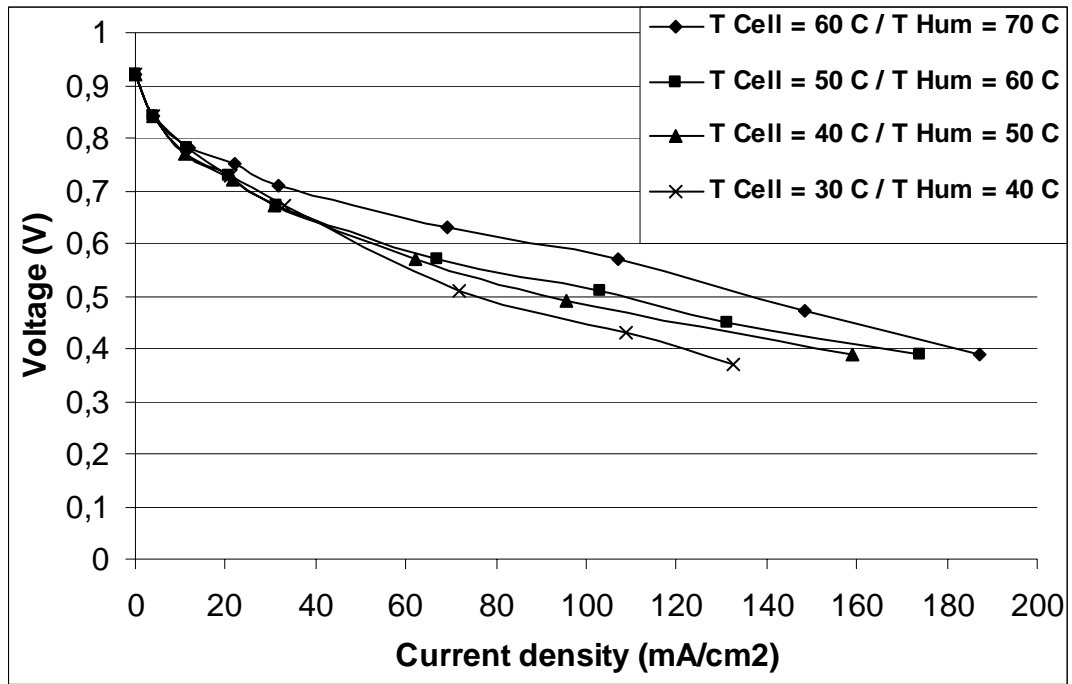


Figure 4.4 Effect of cell temperature at high humidification level

(T Hum = T Cell + 10 °C; H₂: 0.1 sLm; O₂:0.05 sLm)

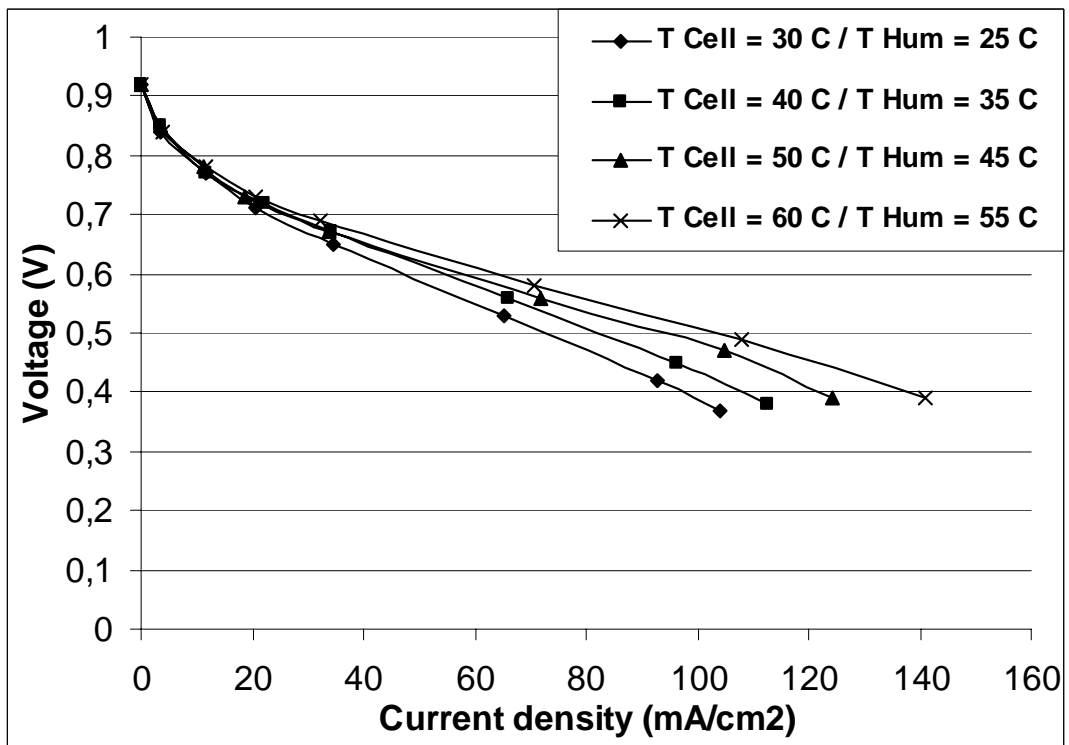


Figure 4.5 Effect of cell temperature at low humidification level

(T Hum = T Cell - 5 °C; H₂: 0.1 sLm; O₂: 0.05 sLm)

Increasing cell temperature shifts the performance curves up. In either high humidification or low humidification level maximum performance is observed at 60 °C. On the other hand, there is a significant performance difference between two conditions. At high humidification level AOY001 delivered a current density of 137 mA/cm² at 0.5 V at a cell temperature of 60 °C. At the same cell temperature but with low humidification level, this time AOY001 delivered 105 mA/cm². A higher humidification temperature than the cell temperature favors the performance. This difference applies for all temperatures.

4.2.3 Effect of oxygen to hydrogen ratio

Figure 4.6 shows the effect of oxygen to hydrogen ratio on the performance of AOY001. Performance increases with increasing ratio of oxygen to hydrogen. However, this increase was observed up to an extent. The performance curves with an oxygen flow rate of 0.08 sLm and 0.1 sLm at a hydrogen flow rate of 0.1 sLm kept constant are almost same with each other. Increasing the oxygen flow rate from 0.08 sLm to 0.1 slm did not make a significant performance improvement. AOY001 delivered a current density of 183 mA/cm² at 0.5 V at both conditions.

4.3 Power and efficiency of the AOY001

Power of a fuel cell system can be found as follows

$$P = VI \text{ [2.30]}$$

where V is the operating voltage in volts and I is the current drawn from the fuel cell in amperes. P is in watts. This equation holds for any electrical energy producing system.

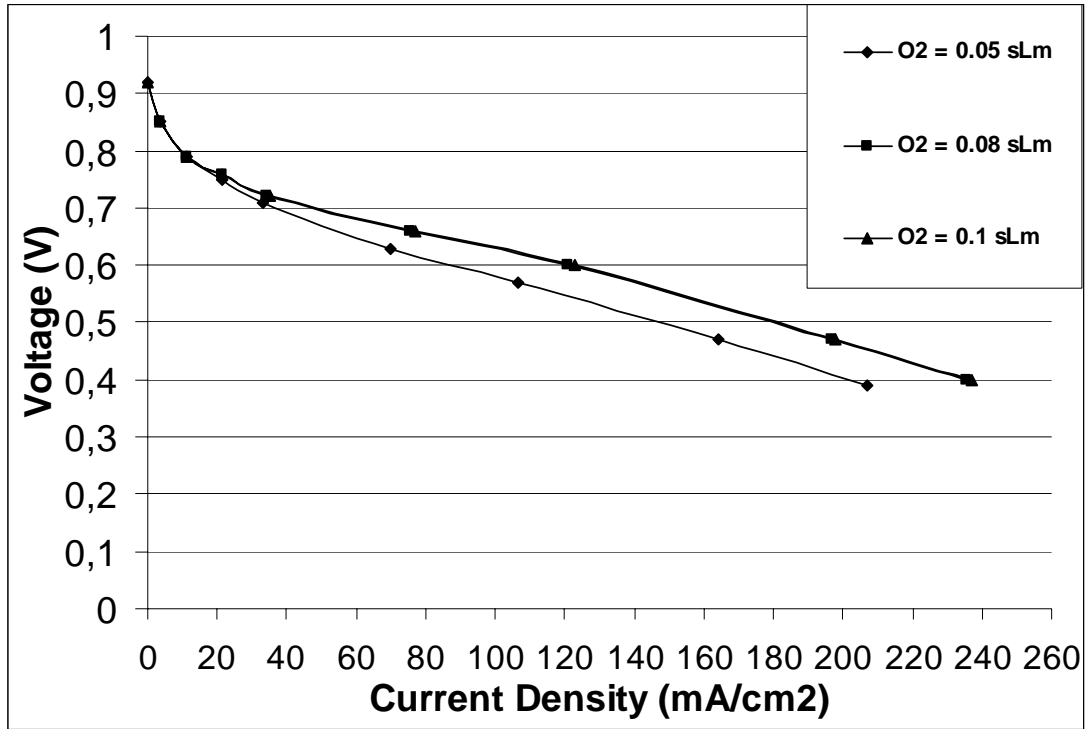


Figure 4.6 Effect of volumetric flow rate ratio of O₂ to H₂

(T Cell = 60 °C; T Hum = 70 °C; H₂: 0.1 sLm)

Therefore, to calculate the power delivered by AOY001, its characteristic V-i curve can be utilized at any conditions. Power at any point can be obtained by multiplying the current density with the active area of the fuel cell and multiplying the resulting value with the corresponding voltage. From the performance figures it can be concluded that AOY001 reached its maximum performance at a cell temperature of 60 °C, a gas humidification temperature of 70 °C and at hydrogen and oxygen flow rates of 0.1 sLm both. Figure 4.7 shows power delivered by AOY001 and voltage-total current curve at the conditions it reached its maximum

performance. Sample calculations to obtain the power values can be found in Appendix A.

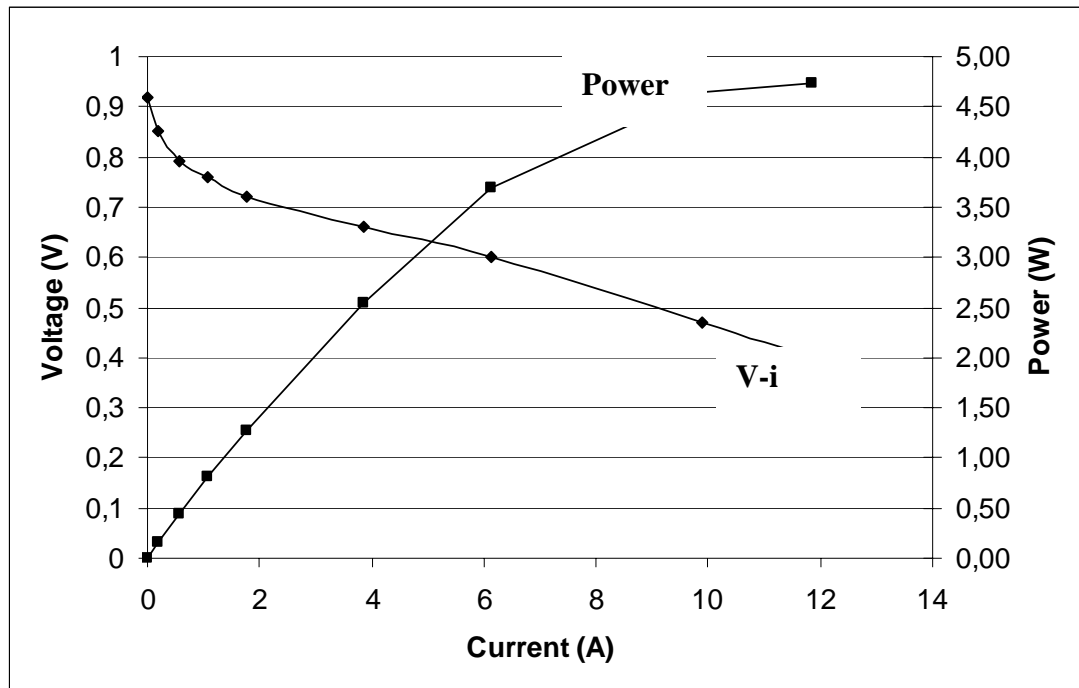


Figure 4.7 Power and voltage-total current curve of AOY001
(T Cell = 60 °C; T Hum = 70 °C; H₂: 0.1 sLm O₂: 0.1 sLm)

As seen from Figure 4.7 a maximum power value of 4.75 W is obtained at 0.4 V. However, this is a misleading result. Because, the slope of the power curve is decreasing as the voltage drops and as the total current drawn from the fuel cell increases. Especially after 0.6 V inclination is higher. This is also an indication that efficiency of the fuel cell is decreasing. According to Equation 2.29 fuel cell efficiency is directly proportional to the operating voltage and as it decreases so the efficiency does. To draw more current more hydrogen is needed and drawing more current drops operating voltage. At low voltages electrical efficiency decreases and most of the hydrogen is dissipated as heat energy. In other words hydrogen is not

converted to electrical energy as much as it is converted at lower currents. Therefore, it is efficient to operate PEMFCs not below 0.6 V where usually the power curve starts to incline. This is also the point where the ohmic losses are the main concern for the voltage drop. If we try to visualize the electrical resistance of a conductor as the friction that it applies to the electrons flowing through its body, as the flow rate of electrons increase so the friction does. Operating at lower voltages to obtain high power rates is not logical because the fuel is wasted. Instead, fuel cells are connected in series to obtain more power; however, this subject is beyond the scope of this study.

4.4 Comparison of the performances with literature

MEA used in the structure of AOY001 was purchased from Ion-Power. The manufacturer company had their MEAs tested by a fuel cell testing company “Fuel Cell Energy” and they provide the V-i diagram obtained when the was purchased. This V-i diagram is given in Appendix C. In Figure 4.8 for comparison purpose V-i curves supplied by Ion-Power and the one obtained in this at similar conditions were plotted on the same graph. The V-i curve provided by Ion-Power obtained at 60 °C fuel cell temperature, and operated with hydrogen and air with a relative humidity of 100%. V-i curve which was obtained in this study and plotted on Figure 4.8 was studied at 60 °C fuel cell temperature and 70 °C gas humidification temperatures. It is clear that the curve provided by Ion-power presents significantly a better performance although the same MEA was used in both performance tests. This

shows the critical importance of other parts of the PEMFC on the performance.

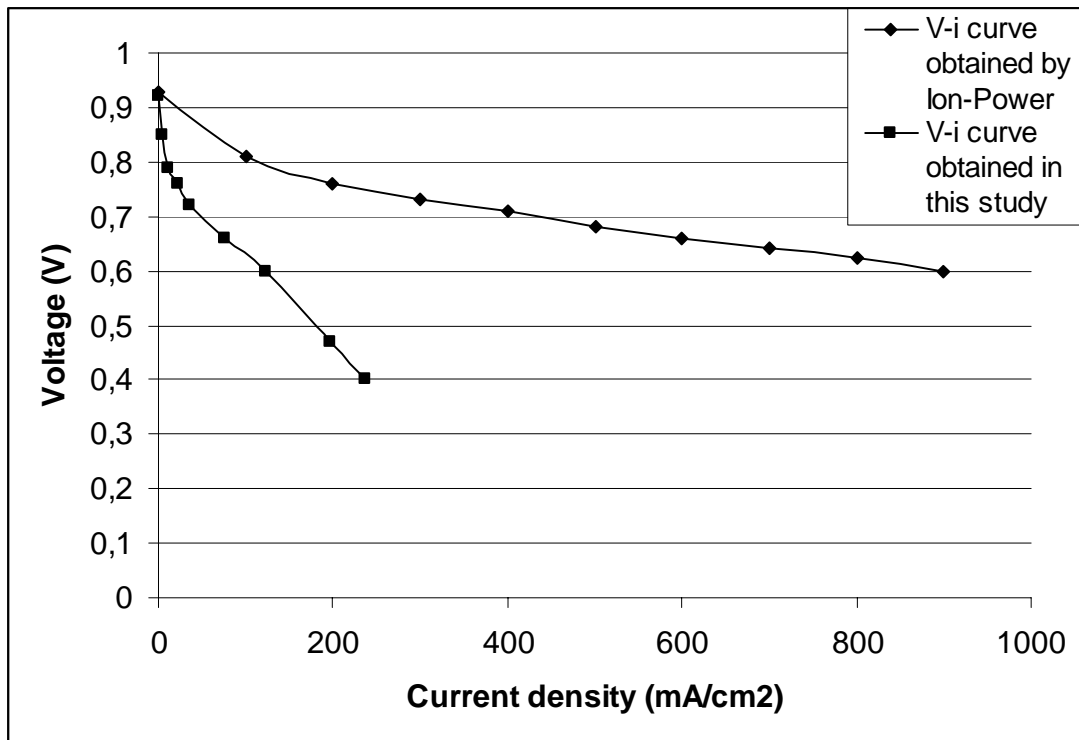


Figure 4.8 Comparison of the V-i curves provided by Ion-Power and obtained in this study of the MEA used in AOY001.

4.5 Discussion

By looking at Figure 4.1 and Table 4.1 it can be concluded that the best performance is obtained from AOY001 and the worst is from EAE1. Among those five fuel cells it is logical to compare EAE1, AOY003 and AOY004 as one group and AOY001 and AOY002 as another group. Because MEAs of EAE1, AOY003 and AOY004 were manufactured in our laboratory and MEAs of AOY001 and AOY002 were purchased.

Although AOY003 has a much lower loading of platinum it presents a better performance. Here the manufacturing method of the MEA could be the main reason for an improved performance. Spraying method provides a more homogenous catalyst layer structure where the platinum particles are distributed all over the surface. Once the reactant gases reach the catalyst layer they react more effectively. Another benefit of the spraying method comes with the thinner catalyst layer formed compared with the catalyst layer formed with rolling method. Thinner layer allows the formation of Nafion-catalyst interphase which is crucial for the protons produced. They should be transferred through the membrane to the cathode side. If a catalyst surface does not contact with Nafion it means that the proton is wasted. Therefore, catalyst particles should be connected to the Nafion membrane by Nafion particles. This kind of structure can be achieved with a thinner catalyst layer more easily. Thinner catalyst layer has also a less resistance which lowers the ohmic loss.

The MEA of AOY004 was also manufactured by spraying method and has a much higher amount of platinum loading. When the V-i curves of two PEMFCs compared the significant performance difference can be best explained by higher platinum loading of AOY003. Catalyst loading is the key material for the fuel cell reaction to take place.

The main problem for the spraying method applied is that while manufacturing it is not possible to control the transfer of the catalyst layer from the Teflon films to the Nafion membrane. During the manufacture of AOY003 and AOY004 sufficient amount of catalyst layer material was sprayed over the Teflon films used to maintain a platinum loading of 0.3 mg/cm^2 and 1 mg/cm^2 respectively. However, a considerable amount of the catalyst layer was not transferred to the

Nafion membrane in both fuel cells.

The main difference between AOY001 and AOY002 is the type of graphite used. The one used in AOY001 supplied by SGL Carbon GmbH is high-purity-graphite and specially developed for fuel cell applications by the manufacturer company. Its conductivity is high and vulnerable to diffusion of reactant gases. On the other hand, the graphite plate used in AOY002 supplied by Morgan Carbon is a kind of material widely used in electrical motors as a brush. Its purity is lower and has a more porous structure. The structural difference between two types of graphite plates mostly affects its electrical conductivity. Materials used in the PEMFCs should possess high electrical conductivity. This could be the main difference which creates the better performance of AOY001 to AOY002. Therefore, materials specially developed for fuel cell applications should be preferred to ensure the high electrical conductivity.

Another worthy comparison is between AOY001 and AOY004. These are the two best PEMFCs where AOY001 presents a better performance. They are quite similar in structure and the amount of catalyst loading. The main difference is the method and membrane type used to manufacture MEAs. Manufacturing method of the MEA is not known since Ion Power who supplied the MEA does not release the method to the public information. However, it is well known that spraying method is widely used to manufacture commercial MEAs by MEA manufacturing companies; although different companies apply different procedures during the steps of manufacturing facility. Considering that the manufacturer company has more experience and advanced equipments to manufacture MEAs, it is reasonable to assume that partly AOY001's performance can be related to this fact. However, this

is not the only and main reason for AOY001's superior performance to AOY004. The main reason is the thickness of the membranes used. AOY001 has a membrane with a thickness of 25 μm , on the other hand AOY004 has a membrane thickness of 125 μm . The transference of protons through the membrane is basically a diffusion process although the phenomenon is too complex which can not be modeled by the simple Fickian diffusion law. But after all this is a diffusion process and it strictly depends on the diffusion path. When the electrochemical reaction is considered which completes at the cathode it is clear that protons and electrons freed from anode side have to meet at the cathode. Electrons travel with a speed which is close to the speed of light; therefore, it would be nonsense to blame the electrons with slowing down the reaction. However, protons diffuse with a speed which is even not comparable to the speed of electrons. As a result thinner the membrane is faster the reaction is and high reaction rate means high performance. Finally, it might be well assumed that if a thinner membrane were used in the manufacture of AOY004 it would probably present a better performance close to AOY001.

A final remark on the structure of the PEMFCs constructed is on the casing material. Except AOY001 all other PEMFCs were constructed by using steel. Kestamid was used in AOY001 as the casing. It is a light and strong material; however, its thermal conductivity is low. Therefore, after AOY001 showed the best performance and chosen to be used during the parametric studies its casing was replaced by steel plates identical to other ones. Because it is not possible to control properly the cell temperature with a Kestamid casing with external heating.

The positive effect of increasing humidification temperature can clearly be seen at Figures 4.2 and 4.3. For the transportation of protons through the membrane

water is acting as the carrier molecule. Therefore the membrane should be wetted sufficiently. As the temperature is increased in the water bath, humidity of gases increases carrying more water inside the cell. When two figures are compared it can be clearly realized that cell performance is low with the excess flow rate of gases. When the gas flow rate is fast, the contact time is not enough for sufficient humidification. Therefore, the gases are not humidified as much as they are humidified in low flow rates. When the gases are not sufficiently humidified, they may cause the membrane to dry up too much which result in low performance.

Figures 4.4 and 4.5 show that increase in the cell temperature had a positive effect on the performance at both high and low humidification conditions. Since the reaction taking place in the PEMFC is basically an oxidation reaction, the kinetics is positively affected in the case of a temperature increase as long as there is sufficient humidification. If sufficient humidification is not provided then increasing temperature will have an adverse effect since the membrane is dried. The overall phenomena taking place within the MEA is strictly limited by the diffusion of protons through the membrane.

Increasing the O₂ to H₂ ratio had also a positive effect on the performance. It is well known that the cathode reaction, which is the reduction of oxygen, has a low rate of kinetics when compared with the anode reaction, hydrogen oxidation. A higher amount of O₂ might have affected the kinetics of the O₂ reduction in a positive way resulting in a higher performance. On the other hand, this positive effect of the increasing flow rate of O₂ has a limit as can be seen from Figure 4.6. An increase of the flow rate from 0.08 sLm to 0.1 sLm did not make any significant improvement on the performance.

Finally, the significant difference between the performances of the same MEAs tested by different test fuel cells in Figure 4.8 is a proof that although MEA is the heart of a PEMFC, other parts also have a critical role on the performance. Therefore, it is a must that the test cell should be improved for further studies.

CHAPTER 5

CONCLUSION AND RECOMMENDATIONS

In this study five H₂/O₂ PEMFCs; EAE1, AOY001, AOY002, AOY003, AOY004 which have different structures and manufacturing methods were constructed. A test station was built to make the performance tests of the PEMFCs. The test station built was capable of regulating the hydrogen and oxygen gas flow rates and controlling the fuel cell temperature and gas humidification temperature. After the primary performance tests which were performed at 25 °C, fuel cell and gas humidification temperature a comparison between the V-i diagrams obtained during the tests revealed that AOY001 was the fuel cell which showed the best performance. AOY001 had a MEA manufactured by Ion Power, GDL 10 BA gas diffusion layers manufactured by SGL Carbon, BPP4 type graphite plates supplied by SGL Carbon with serpentine type flow fields machined over it and a Kestamid casing. AOY001 was chosen to perform the further studies to investigate the effect of different parameters on the performance. Kestamid casing of AOY001 was replaced by steel casing to enable temperature controlling of the fuel cell. These parameters were fuel cell and gas humidification temperature and different flow rates of reactant gases. A standard protocol was used to obtain the V-i diagrams during the tests.

It was found that increasing fuel cell and gas humidification temperatures increased the performance. Excess flow rate of reactant gases had an adverse

effect on the performance. On the other hand increasing the ratio of flow rate of oxygen to hydrogen increased the performance but it did not have any effect after a certain flow rate. This ratio could also be increased keeping the oxygen flow rate constant but decreasing hydrogen flow rate. Then, one would have got a better insight of the process.

The most important outcome of this study was to learn and understand the structure, manufacturing methods, operating principles and testing procedures of PEMFCs and the successful operation of PEMFCs with H₂ and O₂. This study was completely a learning process. Considering the available infrastructure in the laboratory where this study was completed; the experience obtained was a significant contribution to the development of the laboratory and the future studies on the PEMFCs at the laboratory.

An experimental study on a PEMFC may be divided into two parts. The first one is the development of the structure. The heart of a PEMFC is the MEA. This is the place where all the electrochemical reaction coupled with mass transfer is occurring. MEA manufacturing method should either be developed or changed drastically to obtain higher performances. Beside that it should be kept in mind that while developing a method to manufacture an MEA, smaller areas should be preferred. Because materials used are very expensive and even to manufacture a single MEA one may need to spend lots of money.

Another important part of the structure is the gas distribution plates which were graphite in this study. Ohmic loss is one of the main reasons that lowers the operating voltage and the interphase between gas distribution plates and gas diffusion layers is a critical surface where a significant ohmic loss can be observed. On the

other hand, since the test fuel cell may be assembled and disassembled frequently graphite seems not to be the suitable material for test cells. Because graphite is brittle and it may be damaged easily. To reduce ohmic losses and any damage, metal plates can be used instead of graphite plates. Stainless steel is a good candidate for this mission. Furthermore this metal can be coated with a noble metal such as gold or silver to increase the conductivity.

Gas distribution channels are also important on the performance of the PEMFCs. The geometry and the shape of the flow field are here two parameters that might be investigated. However, investigation of this issue where usually CFD methods are used should be handled separately and is usually beyond the scope of developing MEAs. During the development of an MEA a well known reported flow field geometry and shape should be chosen to obtain reliable results.

The second part of the experimental study is the test station. There are some modifications that could be made to improve the test station used in this study. Temperature control of the test fuel cell was accomplished by wrapping a heating band over the PEMFC. However, since a thick insulation plastic was placed between the casing and the conducting parts of PEMFC, a lag occurs between the set temperature and real temperature and temperature control becomes difficult. Instead of this method heating of the PEMFC should be done by heating directly the gas distribution plates where one has direct contact with the MEA and gas diffusion layers.

A pressure control mechanism should also be maintained within the test station since pressure is also an important factor. Two back pressure regulators that would be placed at the gas exits of PEMFC can be employed for this. Sealing should

also be checked for operations under higher pressures.

Finally two gas mass flow meters (not mass flow controllers) should be placed again at the gas exits of the PEMFC to monitor the unreacted gases. This would be very useful to investigate the efficiency and to determine the optimum feed flow rate.

REFERENCES

- Appleby, A.J., Foulkes, F.R., "Fuel Cell Handbook", Van Nostrand, New York, 1989.
- Bockris, J.o'M., Reddy, A.K.N., "Modern Electrochemistry", Vol. 2, Plenum Press, New York, 1970.
- Fedkiw, P.S., Liu, R., Her, W.H., "Insitu electrode formation on a nafion membrane by chemical platinization", Journal of the Electrochemical Society, 139 (1): 15-23, Jan 1992.
- Gierke, T.D., Munn, G.E., Wilson, F.C., "The morphology in nafion perfluorinated membrane products, as determined by wide-angle and small-angle x-ray studies", J Polym Sci Pol Phys, 19 (11): 1687-1704, 1981.
- Giorgi, L., Antolini, E., Pozio, A, et al., "Influence of the ptfe content in the diffusion layer of low-Pt loading electrodes for polymer electrolyte fuel cells", Electrochimica Acta, 43 (24): 3675-3680, 1998.
- Glasstone, S., Laidler K.J., Eyring, H., "The Theory of Rate Processes", McGraw-Hill, New York, 1941, p. 552.
- Gottesfeld, S., Zawodzinski, T.A., in: Alkire, R., Gerischer, H., Kolb, d., Tobias, C., (eds.), "Advances in Electrochemical Science and Engineering", Vol. 5, 1998, 197.
- Gomez, Y.E.C., "Membrane humidification optimization in proton exchange membrane fuel cells", Ms. ,Thesis, University of Puerto Rico, 2001,.
- Grot, W., "Encyclopedia of Polymer Science and Engineering", Vol. 16, 2nd edition, 1989.
- Han, E., "Amelioration of electrodes in alkaline fuel cells", MS. ,Thesis, Middle East Technical University, 2001.
- Han, E., Eroğlu, I., Türker, L., Performance of an alkaline fuel cell with single or double layer electrodes", Int J Hydrogen Energy, 25 (2): 157-165, Feb 2000.
- Haug, A., "Development of low-loading, carbon monoxide tolerant PEM fuel cell electrodes", PhD Thesis, University of South Carolina, 2002, 1-5.

Hoffman, P., "Daimler Benz to unveil world's first fuel cell passenger car this month", *Hydrogen & Fuel Cell Letter*, May 1996.

Kim, J., Lee, S.M., Srinivasan, S., et al., "Modeling of proton-exchange membrane fuel-cell performance with an empirical-equation", *J Electrochem Soc*, 142 (8): 2670-2674, Aug 1995.

Kordesch, K.; Simader, G., "Fuel cells and their applications", VCH, Newyork, 1996.

Larminie, J., Dicks, A., "Fuel Cell Systems Explained", 2nd ed., John Wiley and Sons, London, 2003.

Laurencelle, F., Chanine, R., Hamelin, J., Fournier, M., Bose, T.K., and La Perriere, A., "Characterization of a Ballard MK5-E proton exchange membrane stack", *Fuel Cells*, 1 (1):66-71, 2001.

Moreira, J., Ocampo, A.L., Sebastian, P.J., et al., Influence of the hydrophobic material content in the gas diffusion electrodes on the performance of a pem fuel cell", *Int J Hydrogen Energ*, 28 (6): 625-627 Jun 2003.

Paganin, V.A., Ticianelli, E.A, Gonzalez, E.R., "Development and electrochemical studies of gas diffusion electrodes for polymer electrolyte fuel cells", *J Appl Electrochem*, 26 (3): 297-304, Mar 1996.

Phillip, D., "Chrysler jump starts fuel cell concept", *Detroit News*, Detroit, Michigan, 1997.

Raistrick, D., in: Van Zee, J.W., White, R.E., Kinoshita, K., Burnery, H.S., (eds.), "Proceedings of the symposium on diaphragms, separators, and ion-exchange membranes", The electrochemical society, Pennington, NJ, Vols. 13-86, 1986, 172.

Ren, X.M., Gottesfeld, S., "Electro-osmotic drag of water in poly(perfluorosulfonic acid) membranes", *J Electrochem Soc*, 148 (1): 87-93, Jan 2001.

Rose, B., "GM Promises production ready fuel cell vehicle by 2004", *Fuel Cell 2000*. 1998.

Schroll, C., "Fuel cell power systems for UUVs", *Sea Technology*, 60-61, 1994.

Thampan, T., Malhotra, S., Zhang, J.X., et al., "Pem fuel cell as a membrane reactor", *Catal Today*, 67 (1-3): 15-32, May 15 2001.

Thampan, T., Malhotra, S., Tang, H., et al., "Modeling of conductive transport in proton-exchange membranes for fuel cells", *J Electrochem Soc*, 147 (9): 3242-3250, Sep 2000.

Tomantschger, K., McClusky, F., Oporto, L., et al., "Development of low-cost alkaline fuel-cells", *J Power Sources*, 18 (4): 317-335, Nov 1986.

Tonkovich, A.Y., Zilka, J.L., Lamont, M.J., et al., "Microchannel reactors for fuel processing applications. I. Water gas shift reactor", *Chem Eng Sci* 54 (13-14): 2947-2951, Jul 1999.

Uchida, M., Aoyama, Y., Eda, N., Ogawa, M., "Solid polymer type fuel cell and method for manufacturing the same", *J Power Sources*, 63, (2): 285, December 1996.

Verbrugge, M.W., "Selective electrodeposition of catalyst within membrane electrode structures", *J Electrochem Soc*, 141 (1): 46-53, Jan 1994.

Wilson, M.S., Gottesfeld, S., "High-performance catalyzed membranes of ultra-low Pt loadings for polymer electrolyte fuel-cells", *J Electrochem Soc* 139 (2): 128-130, Feb 1992.

Wilson, S., "Membrane catalyst for fuel cells", US Patents, 5,211,984, May 18 1993.

Wood, D.L., Yi, Y.S., Nguyen, T.V., "Effect of direct liquid water injection and interdigitated flow field on the performance of proton exchange membrane fuel cells", *Electrochimica Acta*, 43 (24): 3795-3809, 1998.

Zawodzinski, T.A., Derouin, C., Radzinski, S, et al., "Water-uptake by and transport through Nafion117 membranes.

APPENDIX A

SAMPLE CALCULATION FOR FUEL CELL POWER

Table A.1 Power values for AOY001

| Voltage (V) | Current density (mA/cm²) | Current (A) | Power (W) |
|------------------------|--|------------------------|----------------------|
| 0.92 | 0 | 0 | 0 |
| 0.85 | 3.8 | 0.19 | 0.16 |
| 0.79 | 11.2 | 0.56 | 0.44 |
| 0.76 | 21.40 | 1.07 | 0.81 |
| 0.72 | 35.20 | 1.76 | 1.27 |
| 0.66 | 77 | 3.85 | 2.54 |
| 0.6 | 122.8 | 6.14 | 3.68 |
| 0.47 | 197.8 | 9.89 | 4.65 |
| 0.4 | 237.4 | 11.87 | 4.75 |

$$\text{Power (W)} = \text{Voltage (V)} \times \text{Current density (mA/cm}^2\text{)} \times \text{Electrode area (cm}^2\text{)} / 1000$$

$$\text{Power (W)} = \text{Voltage (V)} \times \text{Current (A)}$$

$$\text{Maximum power} = 4.75 \text{ W}$$

APPENDIX B

V-i DIAGRAMS OF PARAMETRIC EXPERIMENTS OF AOY001

Table B.1 Effect of humidification temperature with excess flow rate of gases

| T Cell = 50 °C T Hum = 35 °C H ₂ Flow rate = 0.4 sLm O ₂ Flow rate = 0.2 sLm | |
|---|---------------------------------------|
| Voltage (V) | Current density (mA/cm ²) |
| 0,9 | 0,00 |
| 0,82 | 2,00 |
| 0,76 | 5,60 |
| 0,68 | 15,60 |
| 0,59 | 27,80 |
| 0,48 | 48,00 |
| 0,38 | 64,20 |
| T Cell = 50 °C T Hum = 40 °C H ₂ Flow rate = 0.4 sLm O ₂ Flow rate = 0.2 sLm | |
| Voltage (V) | Current density (mA/cm ²) |
| 0,9 | 0,00 |
| 0,83 | 2,00 |
| 0,73 | 8,80 |
| 0,66 | 19,20 |
| 0,51 | 44,40 |
| 0,46 | 55,00 |
| 0,34 | 78,20 |

Table B.1 continued

| T Cell = 50 °C T Hum = 45 °C H ₂ Flow rate = 0.4 sLm O ₂ Flow rate = 0.2 sLm | |
|---|---------------------------------------|
| Voltage (V) | Current density (mA/cm ²) |
| 0,91 | 0,00 |
| 0,84 | 2,80 |
| 0,72 | 12,20 |
| 0,58 | 34,40 |
| 0,5 | 50,00 |
| 0,46 | 60,60 |
| 0,4 | 93,00 |
| T Cell = 50 °C T Hum = 50 °C H ₂ Flow rate = 0.4 sLm O ₂ Flow rate = 0.2 sLm | |
| Voltage (V) | Current density (mA/cm ²) |
| 0,92 | 0,00 |
| 0,8 | 2,60 |
| 0,73 | 9,60 |
| 0,68 | 16,20 |
| 0,57 | 38,40 |
| 0,49 | 57,40 |
| 0,43 | 92,00 |
| 0,37 | 112,8 |
| T Cell = 50 °C T Hum = 55 °C H ₂ Flow rate = 0.4 sLm O ₂ Flow rate = 0.2 sLm | |
| Voltage (V) | Current density (mA/cm ²) |
| 0,91 | 0,00 |
| 0,83 | 3,20 |
| 0,74 | 15,20 |
| 0,69 | 27,80 |
| 0,58 | 54,60 |
| 0,54 | 69,80 |
| 0,44 | 102,20 |
| 0,38 | 118,2 |

Table B.1 continued

| T Cell = 50 °C T Hum = 60 °C H ₂ Flow rate = 0.4 sLm O ₂ Flow rate = 0.2 sLm | |
|---|---------------------------------------|
| Voltage (V) | Current density (mA/cm ²) |
| 0,9 | 0,00 |
| 0,84 | 3,20 |
| 0,76 | 14,40 |
| 0,72 | 23,80 |
| 0,67 | 34,00 |
| 0,57 | 71,80 |
| 0,47 | 114,40 |
| 0,37 | 139,4 |

Table B.2 Effect of humidification temperature

| T Cell = 50 °C T Hum = 60 °C H ₂ Flow rate = 0.1 sLm O ₂ Flow rate = 0.05 sLm | |
|--|---------------------------------------|
| Voltage (V) | Current density (mA/cm ²) |
| 0,92 | 0,00 |
| 0,84 | 3,60 |
| 0,78 | 14,60 |
| 0,75 | 23,00 |
| 0,71 | 38,60 |
| 0,63 | 70,20 |
| 0,55 | 105,80 |
| 0,45 | 148,6 |
| 0,39 | 172,6 |

Table B.2 continued

| T Cell = 50 °C T Hum = 55 °C H ₂ Flow rate = 0.1 sLm O ₂ Flow rate = 0.05 sLm | |
|--|---------------------------------------|
| Voltage (V) | Current density (mA/cm ²) |
| 0,93 | 0,00 |
| 0,84 | 4,20 |
| 0,77 | 14,60 |
| 0,73 | 22,60 |
| 0,67 | 36,20 |
| 0,6 | 67,80 |
| 0,54 | 99,40 |
| 0,45 | 139,2 |
| 0,39 | 162,4 |
| T Cell = 50 °C T Hum = 50 °C H ₂ Flow rate = 0.1 sLm O ₂ Flow rate = 0.05 sLm | |
| Voltage (V) | Current density (mA/cm ²) |
| 0,92 | 0,00 |
| 0,85 | 3,60 |
| 0,77 | 14,60 |
| 0,73 | 22,00 |
| 0,68 | 33,80 |
| 0,57 | 65,80 |
| 0,51 | 94,00 |
| 0,45 | 126,80 |
| 0,37 | 159,20 |
| T Cell = 50 °C T Hum = 45 °C H ₂ Flow rate = 0.1 sLm O ₂ Flow rate = 0.05 sLm | |
| Voltage (V) | Current density (mA/cm ²) |
| 0,92 | 0,00 |
| 0,84 | 3,80 |
| 0,77 | 13,40 |
| 0,72 | 21,80 |
| 0,66 | 34,20 |
| 0,54 | 67,00 |
| 0,43 | 100,60 |
| 0,37 | 122,40 |

Table B.2 continued

| T Cell = 50 °C T Hum = 40 °C H ₂ Flow rate = 0.1 sLm O ₂ Flow rate = 0.05 sLm | |
|--|---------------------------------------|
| Voltage (V) | Current density (mA/cm ²) |
| 0,92 | 0,00 |
| 0,84 | 3,80 |
| 0,78 | 10,20 |
| 0,72 | 19,80 |
| 0,62 | 36,00 |
| 0,54 | 65,60 |
| 0,44 | 95,60 |
| 0,37 | 118,40 |

| T Cell = 50 °C T Hum = 35 °C H ₂ Flow rate = 0.1 sLm O ₂ Flow rate = 0.05 sLm | |
|--|---------------------------------------|
| Voltage (V) | Current density (mA/cm ²) |
| 0,92 | 0,00 |
| 0,84 | 3,60 |
| 0,78 | 11,80 |
| 0,71 | 22,20 |
| 0,64 | 35,20 |
| 0,52 | 65,40 |
| 0,42 | 93,80 |
| 0,37 | 112,20 |

Table B.3 Effect of fuel cell temperature with high level of humidification

| | |
|--|---------------------------------------|
| T Cell = 60 °C T Hum = 70 °C H ₂ Flow rate = 0.1 sLm O ₂ Flow rate = 0.05 sLm | |
| Voltage (V) | Current density (mA/cm ²) |
| 0,92 | 0,00 |
| 0,84 | 3,80 |
| 0,78 | 11,80 |
| 0,75 | 22,20 |
| 0,71 | 31,60 |
| 0,63 | 69,20 |
| 0,57 | 107,20 |
| 0,47 | 148,60 |
| 0,39 | 187,20 |
| T Cell = 50 °C T Hum =60 °C H ₂ Flow rate = 0.1 sLm O ₂ Flow rate = 0.05 sLm | |
| Voltage (V) | Current density (mA/cm ²) |
| 0,92 | 0,00 |
| 0,84 | 3,80 |
| 0,78 | 11,60 |
| 0,73 | 20,80 |
| 0,67 | 31,20 |
| 0,57 | 66,80 |
| 0,51 | 103,00 |
| 0,45 | 131,20 |
| 0,39 | 174,20 |
| T Cell = 40 °C T Hum =50 °C H ₂ Flow rate = 0.1 sLm O ₂ Flow rate = 0.05 sLm | |
| Voltage (V) | Current density (mA/cm ²) |
| 0,92 | 0,00 |
| 0,84 | 3,80 |
| 0,77 | 11,00 |
| 0,72 | 21,80 |
| 0,67 | 31,00 |
| 0,57 | 62,00 |
| 0,49 | 95,40 |
| 0,39 | 159,20 |

Table B.3 continued

| T Cell = 30 °C T Hum =40 °C H ₂ Flow rate = 0.1 sLm O ₂ Flow rate = 0.05 sLm | |
|---|---------------------------------------|
| Voltage (V) | Current density (mA/cm ²) |
| 0,92 | 0,00 |
| 0,84 | 3,80 |
| 0,77 | 11,20 |
| 0,73 | 21,00 |
| 0,67 | 33,00 |
| 0,51 | 71,80 |
| 0,43 | 108,60 |
| 0,37 | 132,40 |

Table B.4 Effect of fuel cell temperature with low level of humidification

| T Cell = 30 °C T Hum =25 °C H ₂ Flow rate = 0.1 sLm O ₂ Flow rate = 0.05 sLm | |
|---|---------------------------------------|
| Voltage (V) | Current density (mA/cm ²) |
| 0,92 | 0,00 |
| 0,84 | 3,40 |
| 0,77 | 11,60 |
| 0,71 | 20,40 |
| 0,65 | 34,60 |
| 0,53 | 65,20 |
| 0,42 | 92,80 |
| 0,37 | 104,20 |

Table B.4 continued

| T Cell = 40 °C T Hum = 35 °C H ₂ Flow rate = 0.1 sLm O ₂ Flow rate = 0.05 sLm | |
|--|---------------------------------------|
| Voltage (V) | Current density (mA/cm ²) |
| 0,92 | 0,00 |
| 0,85 | 3,40 |
| 0,77 | 11,60 |
| 0,72 | 22,00 |
| 0,67 | 34,20 |
| 0,56 | 66,20 |
| 0,45 | 96,20 |
| 0,38 | 112,60 |
| T Cell = 50 °C T Hum = 45 °C H ₂ Flow rate = 0.1 sLm O ₂ Flow rate = 0.05 sLm | |
| Voltage (V) | Current density (mA/cm ²) |
| 0,92 | 0,00 |
| 0,85 | 3,60 |
| 0,78 | 11,40 |
| 0,73 | 18,80 |
| 0,67 | 33,60 |
| 0,56 | 71,80 |
| 0,47 | 104,80 |
| 0,39 | 124,20 |
| T Cell = 60 °C T Hum = 55 °C H ₂ Flow rate = 0.1 sLm O ₂ Flow rate = 0.05 sLm | |
| Voltage (V) | Current density (mA/cm ²) |
| 0,92 | 0,00 |
| 0,84 | 3,80 |
| 0,78 | 11,60 |
| 0,73 | 20,60 |
| 0,69 | 32,20 |
| 0,58 | 70,80 |
| 0,49 | 107,80 |
| 0,39 | 141,00 |

Table B.5 Effect of O₂ to H₂ ratio

| T Cell = 60 °C T Hum = 70 °C H ₂ Flow rate = 0.1 sLm O ₂ Flow rate = 0.05 sLm | |
|--|---------------------------------------|
| Voltage (V) | Current density (mA/cm ²) |
| 0,92 | 0,00 |
| 0,85 | 3,80 |
| 0,79 | 11,20 |
| 0,75 | 21,40 |
| 0,71 | 33,00 |
| 0,63 | 70,00 |
| 0,57 | 106,80 |
| 0,47 | 164,20 |
| 0,39 | 206,80 |
| T Cell = 60 °C T Hum = 70 °C H ₂ Flow rate = 0.1 sLm O ₂ Flow rate = 0.08 sLm | |
| Voltage (V) | Current density (mA/cm ²) |
| 0,92 | 0,00 |
| 0,85 | 3,80 |
| 0,79 | 11,20 |
| 0,76 | 21,40 |
| 0,72 | 34,40 |
| 0,66 | 75,20 |
| 0,6 | 121,00 |
| 0,47 | 197,00 |
| 0,4 | 235,60 |

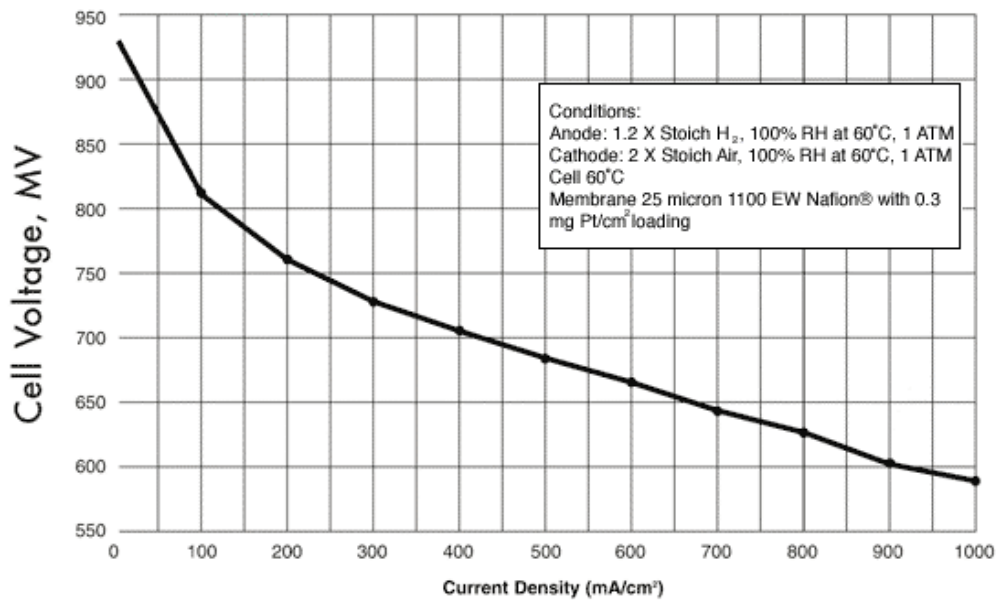
Table B.5 continued

| T Cell = 60 °C T Hum = 70 °C H ₂ Flow rate = 0.1 sLm O ₂ Flow rate = 0.1 sLm | |
|---|---------------------------------------|
| Voltage (V) | Current density (mA/cm ²) |
| 0,92 | 0,00 |
| 0,85 | 3,80 |
| 0,79 | 11,20 |
| 0,76 | 21,40 |
| 0,72 | 35,20 |
| 0,66 | 77,00 |
| 0,6 | 122,80 |
| 0,47 | 197,80 |
| 0,4 | 237,40 |

APPENDIX C

V-i DIAGRAM OF ION-POWER'S MEA TESTED BY FUEL CELL ENERGY

Ion Power, Inc ULTRA THIN MEA PERFORMANCE TEST UNDER
ATOMOSPHERIC CONDITIONS



Testing By:
FuelCell Energy

Figure C.1 V-i diagram of purchased MEA from Ion-Power